MINISTRY OF NATIONAL EDUCATION

THE ANNALS OF "DUNAREA DE JOS" UNIVERSITY OF GALATI

Fascicle IX
METALLURGY AND MATERIALS SCIENCE

YEAR XXXVI (XXXXI)
June 2018, no. 2

ISSN 1453-083X

2018
GALATI UNIVERSITY PRESS

EDITORIAL BOARD

THE ANNALS OF "DUNAREA DE JOS" UNIVERSITY OF GALATI.
FASCICLE IX, METALLURGY AND MATERIALS SCIENCE
Nº. 2 - 2018, ISSN 1453-083X

Table of Contents

THE ANNALS OF "DUNAREA DE JOS" UNIVERSITY OF GALATI.
FASCICLE IX, METALLURGY AND MATERIALS SCIENCE
Nº. 2 - 2018, ISSN 1453-083X

THE ANNALS OF "DUNAREA DE JOS" UNIVERSITY OF GALATI.
FASCICLE IX, METALLURGY AND MATERIALS SCIENCE
N°. 2 - 2018, ISSN 1453-083X

IMPACT OF HYDROCARBON EXPLOITATION ACTIVITY ON SURFACE AND UNDERGROUND WATERS IN THE AREA

Viorel DRAGAN, Betrice TUDOR
"Dunarea de Jos" University of Galati, 111 Domnească Street, 800201, Galaţi, Romania
e-mail: vdragan@ugal.ro

ABSTRACT

This paper presents the natural components of water, and those of pollution. For this, water samples were taken from the brook that runs through the analysed area, and from a fountain, located on the edge of the village, near which many wells are located. The result of these analyses was compared with the regulation, which refers to the quality of drinking water, aiming at protecting people against the effects of contamination.

KEYWORDS: hydrocarbon exploitation, water quality, contamination

1. Introduction

Exploitation Independenţa is located on the territory of Galati, on the outskirts of the localities, Schela, Slobozia Conachi and Independenţa, about 22 km away northwest from Galati. The discovery of the oil structure Independența caused the emergence of a field of wells, reservoir parks, oil deposit, and other annexes, as a result, the agricultural preponderance was diminished by the industrial one.

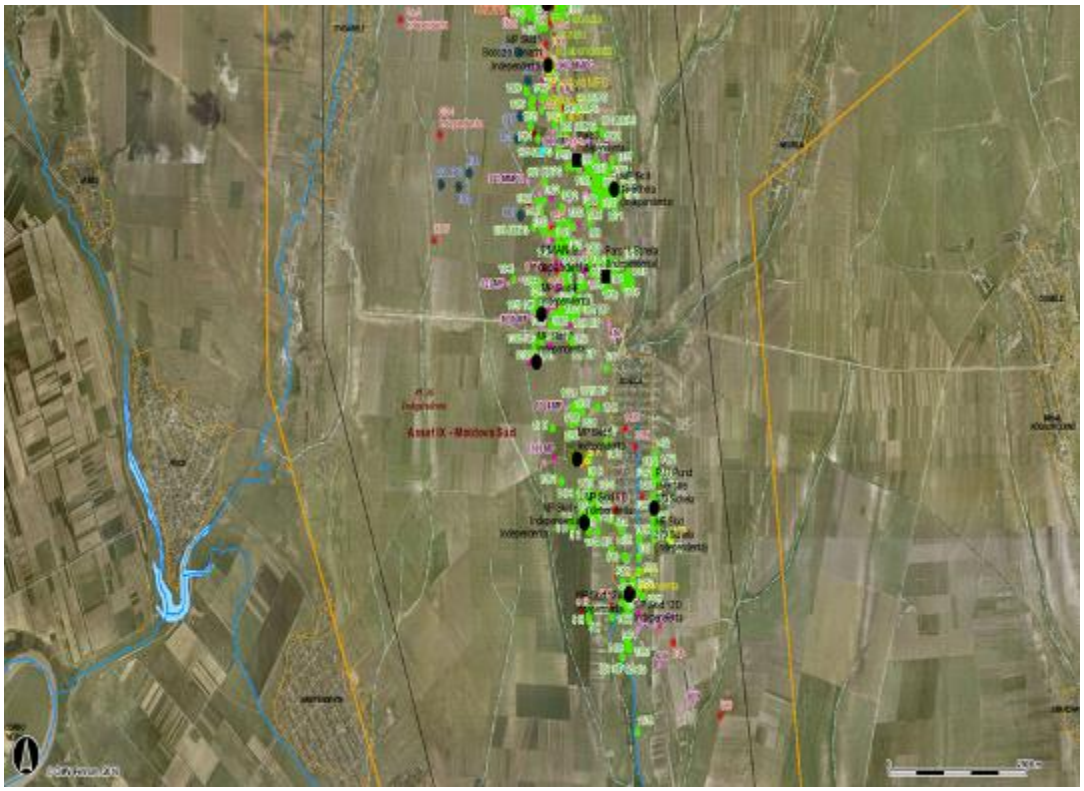

Fig. 1. *GIS Map - Independenţa Oil Zone* [3]

The site is in the river basin of the Siret River, one of the largest rivers in the country, in length, and drained surface. In the area, the hydrographic network is poor, the most important permanent course being the Lozova brook, which collects water from the Căpăţâna Valley, a watercourse, strongly influenced by the precipitation regime. The low volume of precipitation, and the significant level differences, caused the formation of streams, with significant soil erosion, during torrential rains. In this way, many lands are degraded, transformed into pastures [1].

So far, over the Independence structure, more than 800 wells have been dug. Out of these, 420 wells are in operation, and the crude oil flow is about 700 t/day. Wastewater discharge is made by 8 wells [4].

Fig. 2. *Pump unit*

Soil and groundwater pollution can be direct (loss and infiltration of fluids), and indirect (pollutant emissions into the atmosphere, which are worn by wind, are deposited on the soil, where they are washed by precipitation, and infiltrate into the substrate).

By infiltration, of the fertilizers, fungicides for the insect, wastewater and zootechnics, can occur the deep-water pollution. Soil pollution with phenols, cresols, massive residues of petroleum products, leads to the long-term pollution, of the underground water layer with the impossibility of using it [5].

The source of natural pollution, which can cause pollution of surface and underground waters in the Independence oil zone, is the meteoric waters in the form of torrential rains with very high intensities. In this situation, the wells and the parks can be flooded, and subject to partial washing. Surface water, which intercepts the flood, and which transits the land, downstream from parks, to the natural receiver, can suffer both chemical and organoleptic depreciation [2].

2. Determination of water quality

The physicochemical analysis of water aims at determining the natural components of the water, as well as of the pollutants. Water quality control can be done through current, complete or special analyses, depending on the intended purpose [4-6].

Regarding surface water, water samples were taken, outside from the locality, from an area of interest because, in addition to the wells, there is also a park in the area. The two surface water samples were taken as follows: the first sample (A 2) was taken upstream of the park, 50 m away, and the second sample (A 3) was taken downstream, 50 m away from the park.

Regarding groundwater, even if the tanks parks, the oil depot and the annexes related to the Independenta oilfield are on the outskirts of Schela and Slobozia Conachi localities, part of the wells, they reach the neighbourhood of the individual households in Schela. Under these circumstances, a sample of water (A 1) was taken from a village fountain. The water taken from the local fountain is possibly influenced by the activity carried out in the area, considering the probes spreading on the surface of the analysed perimeter, and the underground communication of the permeable porous.

The determinations were made at the Stationary Laboratory for Soil and Water Analysis at Galati Engineering Faculty where the following parameters were determined: pH, turbidity, residual chlorine, hardness, salinity, sulphate, calcium, magnesium.

For the determination of water quality, the stationary laboratory equipment was used to analyse soil and water samples at the Faculty. The analyses were performed with the DR 5000 spectrophotometer, and the portable multiparameter HQ 40d, to determine the pH (Fig. 4, Fig. 5).

After analysis, the samples taken from the Lozova brook will be recorded and compared with the regulations in force concerning the quality of the drinking water (Table 1).

Fig. 3. *Fountain water sampling area (A1)* [3]

Fig. 4. *Spectrophotometer DR 5000* [6]

Fig. 5. *Portable multiparameter HQ 40d* [7]

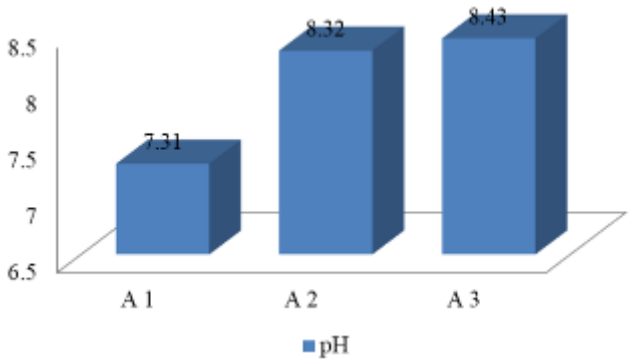

Fig. 6. *pH content of the 3 water samples*

Table 1. *Determinations of the analysed indicators, and their comparison with the laws in force*

Indicator analysed	Unit of measurement	A_1	A_2	A_3	Law 458/2002 Law 311/2004
pH	pH units	7.31	8.32	8.43	6.5 < pH < 9.5
Turbidity	mg/L	1.00	6.00	8.00	<5
Chlorine	mg/L	0.10	0.10	0.10	0.1 < pH < 0.5
Hardness	ppm	41.30	20.30	19.60	5.0
Salinity	‰	12.60	4.49	4.46	-
Sulphate (SO_4^{2-})	mg/L	>3.50	82.00	86.00	250.0
Calcium	mg/L	73.50	78.20	74.90	-
Magnesium	mg/L	134.00	40.40	39.20	-

By analysing each indicator in part, from all three samples taken, we find the following:

• pH - water from the village fountain, has a slightly alkaline character, close to the neutral zone. The two samples taken from the Lozova brook indicate a higher value of alkalinity, exceeding 8 units. However, the value indicated by the regulations in force ranges from 6.5 to 9.5 units, so the pH of the water is ideal and does not seem to be affected by any pollutant;

• turbidity - comparing the three samples taken, we can see that only the water in the well has a degree of transparency, in the normal range of less than 5 units, the other two, exceeding by 1 and 3 units the value required by the regulation. Considering that turbidity is produced, and river deposits, it is possible that this is the main cause of water opacity;

• hardness – it is given by the concentration of calcium and magnesium salts. By comparing the indicated measurement values, we can see that the water in the well exceeds the 8-fold concentration level imposed by the regulations in force. The other two samples, taken from the Lozova brook, exceed the value indicated by the regulation, 5 units, reaching about 20 units. In this case, it is necessary to know the source of the calcium and magnesium salts in the water.

• sulfates - salts of sulfuric acid. The sulphate content of the three samples falls below the limits set by the regulations in force, of 250 units, being quite low in the samples from the Lozova brook, and at a very low level, just 3.5 units at the well water.

• residual Chlorine - The level of chlorine in the water falls within the limits of the law, with an identical value for all three samples taken, of 0.1 mg/L. Since the value indicated by the "Drinking Water Quality" regulations ranges from 0.1 to 0.5 mg/L, we believe that the water in the area under consideration is an ideal one, does not endanger human health, nor does it the environment.

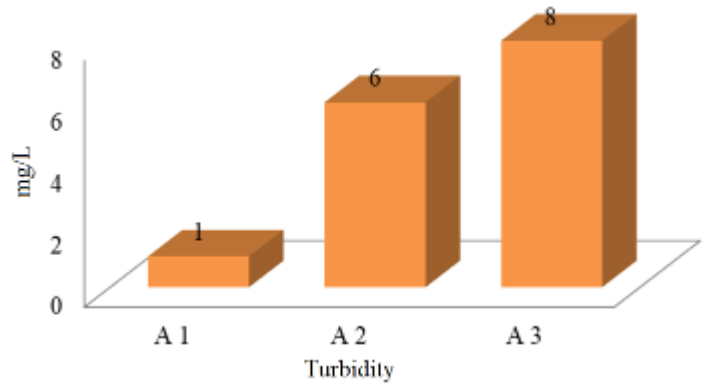

Fig. 7. *Water turbidity in the analysed area*

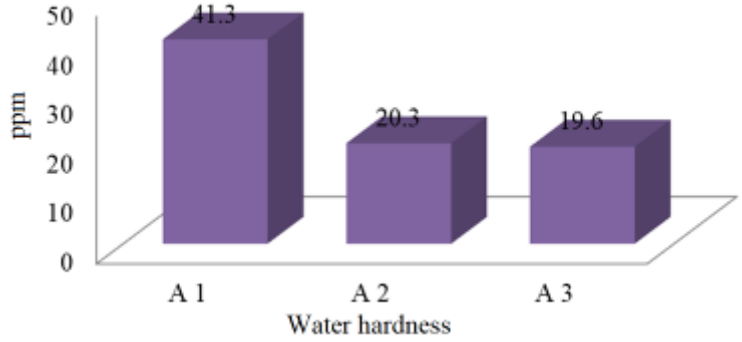

Fig. 8. *Water hardness of samples taken*

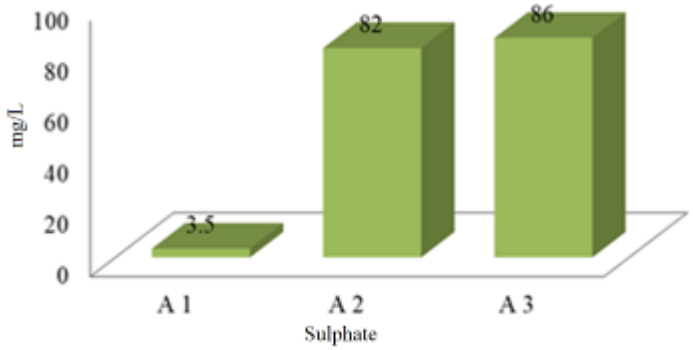

Fig. 9. *Sulphate (SO_4^{2-}) content in water*

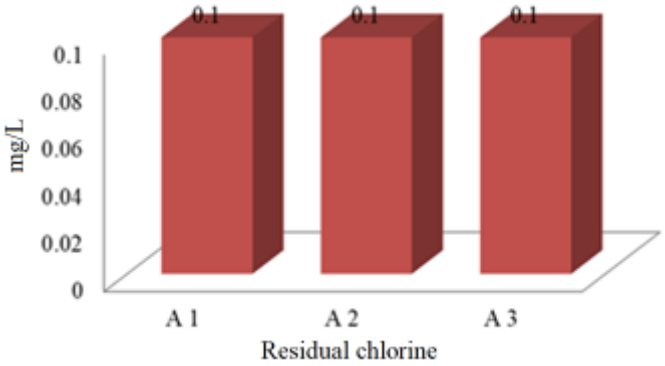

Fig. 10. *Concentration of residual chlorine from the collected water*

3. Conclusions

To analyse the water concentrations, we compared the values recorded by the measuring apparatus with the values indicated by the regulations in force, namely, Law no. 458 of July 8, 2002, regarding the quality of drinking water, and Law no. 311 of 28 June 2004, amending and supplementing Law no. 458/2002 on the quality of drinking water [9].

The present law regulates the quality of drinking water with the objective of protecting human health against the effects of any type of drinking water contamination by ensuring its quality.

As can be seen, the main problem is the high content of calcium and magnesium salts from all three samples, with more emphasis being placed on water in the well, which exceeds 8 times the value required by law. This requires prohibiting the use of that water for drinking purposes, but not its use in irrigating crops.

The analyses on surface and underground water have been designed to determine the natural components of water as well as those of pollution. Samples taken from the brook that runs through the area, and from the fountain, located on the edge of the location where probes are located, indicated quite high values in terms of their hardness. In all three cases, the degree of transparency is exceeded only by the water in the creek. The other indicators correspond to the values indicated by the regulations on water quality.

References

[1]. Baltă Ş., *Tehnici si echipamente pentru tratarea solurilor poluate*, Universitatea Dunarea de Jos, Galati, 2016.
[2]. Popa I., *Colectarea, tratarea şi transportul petrolului şi produselor petroliere din schelele de producţie*, Editura Tehnică şi Pedagogică, Bucureşti, 1985.
[3]. ***, http//gis.petrom.com.
[4]. ***, Arhiva OMV Petrom.
[5]. ***, *Poluarea apei cause, clasificare poluanti consecinte protectie*, http://www.referatele.com/referate/chimie/online7.
[6]. ***, http://www.fmsm.ugal.ro/Mediu-Munteanu.pdf.
[7]. ***, https://www.precisa.ro/produs/multiparametru-hach-hq40d-multi/.
[8]. ***, https://sanatatea.com/pub/mediu/1434-determinarea-calitatilor-fizico-chimice-ale-apei-potabile.html.
[9]. ***, Legea nr. 458 din 8 iulie 2002 privind calitatea apei potabile şi Legea nr. 311 din 28 iunie 2004.

THE ANNALS OF "DUNAREA DE JOS" UNIVERSITY OF GALATI.
FASCICLE IX, METALLURGY AND MATERIALS SCIENCE
N°. 2 - 2018, ISSN 1453-083X

STUDIES AND RESEARCH ON DETERMINING THE CAUSE OF THE CRACKING OF X60 PIPELINE IN THE EXPANDING OPERATION

Stela CONSTANTINESCU
"Dunarea de Jos" University of Galati, Faculty of Engineering, Romania
e-mail: constantinescu_stela@ yahoo.com

ABSTRACT

In this paper was followed the determination of the cause of pipe cracking in the expansion operation. The metallographic analysis of a sample taken from the X60 pipeline was performed to determine the cause of pipe cracking. The structure of the material presents the following defects: linear macro-inclusions type silicates fragile, which layer the material and affect virtually all the thickness of the board; linear segregations in carbon, thickness 0.4-1.5 mm; segregations area in sulphur, and linear segregation in sulphur at the half thickness of the board; in the area of the fissure, the presence of hard particles, with the hardening structure, which influenced the normal flow of steel to deformation. The presence of hard particles, with the hardening structure, in the rift area influenced the normal flow of steel to deformation. The presence of the overlay formed in hot lamination on the surface of the board indicates the existence of a material defect, which changed the normal flow of the material during deformation. At the expansion operation, in the area of overlap of the material, due to these structural inhomogeneities, the limit of breaking resistance was exceeded, and the material was cracked on about 90% of the thickness of the table.

KEYWORDS: segregation in sulphur, macroscopic inclusions, fragile silicates, purity of steel

1. Introduction

In this paper was followed the determination of the cause of the pipe cracking in the expansion operation. The metallographic analysis of a sample taken from the X60 pipeline was performed to determine the cause of the pipe cracking. The presence of hard particles, with the hardening structure, in the rift area influenced the normal flow of steel to deformation. At the expansion operation, in the area of overlap of the material, due to these structural inhomogeneities, the limit of breaking resistance was exceeded, and the material was cracked on about 90% of the thickness of the tablet. This primary segregation in sulphur and phosphorus print a strong character in the strings, the structure of the X60 steel. It was found that at app. 5 mm the outer surface of the board (in the outer overlay area), on the transverse rift, the normal flow of the material to the hot deformation was prevented by the presence of stain particles. These particles still retain the hardening structure, unremoved by hot lamination of the board, due to its characteristics different from those of steel. At the half of the thickness of the board were emphasized segregations area in sulphur, and linear segregation in sulphur. The appearance, nature, location and dimensions of the structural inhomogeneities indicate the faulty leadership of the elaboration-casting stage.

2. Experiments. Analyses carried out

The analysis was carried out on a sample of the well-determined dimensions shown in Figure 1, the sample that comprises the defective area, was taken from a X60 fissured pipe to the expanding operation.

On the surface of the sample and in the section of the table according to Figure 1, the following analyses were performed: 1 - macroscopic analysis on the surface and in the cross section of the sample (section "T " – Figure 1, 2 - The segregation-sulphur footprint, 3 - analysis microscopic (purity of steel in section "L " and structure in section "T " – Figure 1).

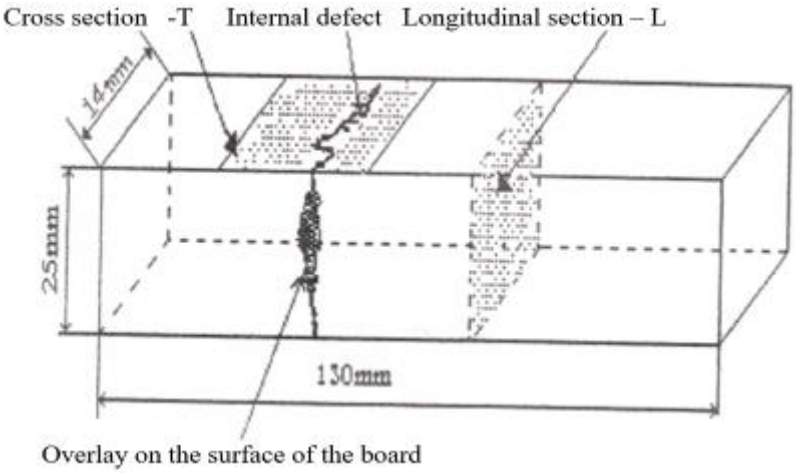

Fig. 1. *Location of the faulty area on the surface of the board and sections "T" and "L" analysed*

3. Results and discussion

3.1. Macroscopic appearance

On the outer surface there is a longitudinal overlap of the material on the entire length of the sample (Figure 2).

The cross section shows, starting from the longitudinal overlay, the zigzag fissure developed, in the analysed plan, on approx. 90% of the thickness of the board. The macroscopic attack with hydrochloric acid indicates linear chemical segregations of different lengths (in the centre of the thickness of the linear segregation table occupying virtually all the length of the sample). The dark aspect of linear segregations indicates the existence of higher carbon content in these areas (Figure 3).

Fig. 2. *Macroscopic issues. Surface of the board-presence of the overlap of material x1,4*

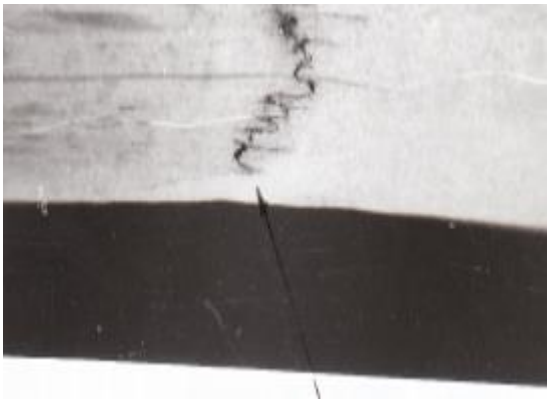

Fig. 3. *Macroscopic issues. Cross section "T" – Fissure area x 1.4*

3.2. Segregation in Sulphur

The Baumann footprint performed in the cross section of the board indicates a non-uniform distribution of sulphur. There is a higher concentration in sulphur on half a sample, which also comprises an area with an abnormal flow of material. In the central area of the thickness of the board is observed a linear segregation in sulphur, on almost the entire length of the cross section (Figure 4).

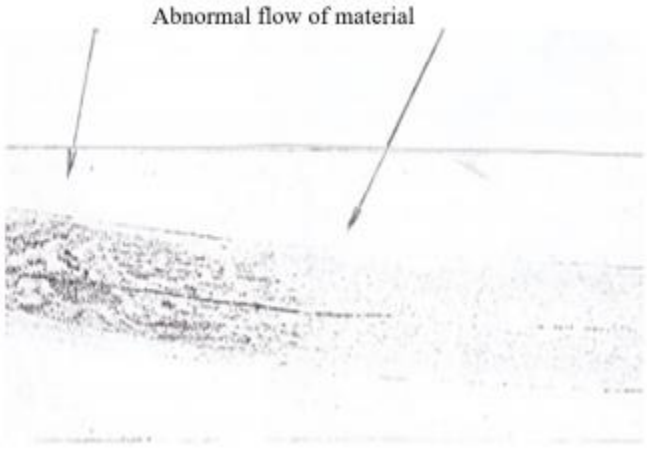

Fig. 4. *Macroscopic issues. Segregation in sulphur – the footprint of Baumann*

3.3. Microscopic analysis

3.3.1. Purity of Steel

The aspects of purity steel were made in macroscopic and microscopic evidence in the longitudinal section "L ". It has been found to have macroscopic inclusions that affect virtually all the thickness of the tablet, in the analysed plan. Recorded macroscopic inclusions are of silicates fragile type (Figure 5).

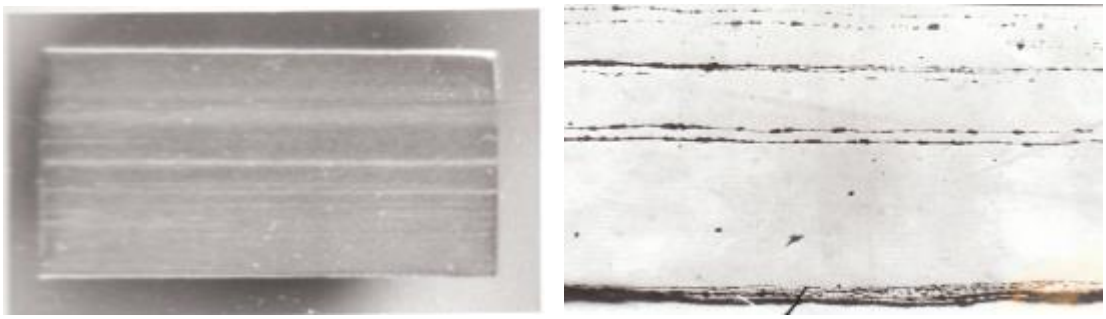

a) aspect macroscopic x3 b) Microscopic appearance x100

Fig. 5. *Aspects of steel purity. Longitudinal section "L"*

3.3.2. Steel structure in defective area

The steel structure in the defective area has been analysed in the cross section "T".

It was found that at approx. 5 mm of the outer surface of the Board (in the outer overlay area), on the transverse rift, the normal flow of the material to the hot deformation was prevented by the presence of foreign particles. These particles still retain the hardening structure, not removed by hot lamination of the board, due to its characteristics different from those of steel. (Figure 6 - detail D).

The steel structure has a strong character in the strings due to the primary segregation in Sulphur and phosphorus, accompanied by the presence of non-metallic inclusions. There were also registered as structural defects, bands having the width of 0.4-1.5 mm in which the larger quantity of Perlite indicated a higher carbon content (segregation area in carbon).

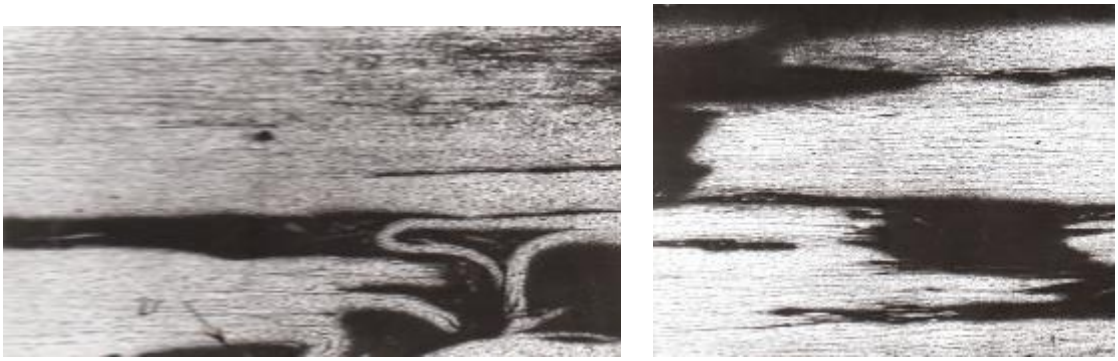

a) macroscopic structure x32 b) microscopic structure x320 (detail in area D)

Fig. 6. *Structural aspects of the section of the board. Cross section "T"*

3. Conclusions

The presence of the overlay formed in hot lamination on the surface of the Board indicates the existence of a material defect, which changed the normal flow of the material during deformation.

The structure of the material shows the following defects:

- fragile macro-inclusions linear silicates types, which layer the material and practically affect all the thickness of the board;
- linear segregations in carbon, with thickness of 0.4-1.5 mm.
- segregations area in sulphur, and linear segregation in sulphur at half thickness of the board.
- in the area of the fissure, the presence of hard particles, with the hardening structure, which influenced the normal flow of steel to deformation.

At the expansion operation, in the area of overlap of the material, due to these structural inhomogeneities, the limit of breaking resistance was exceeded, and the material was cracked on about 90% of the thickness of the table.

The appearance, nature, location and dimensions of these structural inhomogeneities indicate the faulty leadership of the elaboration-casting stage.

References

[1]. Cananau N., Ivanescu A., *Study on the relation between the quality of continuous cast slabs and the surface discontinuities of the steel thick sheet*, 1st International Conference on Advances in Materials and Processing Technologies, Leganes, Madrid, Spain, vol. 2, p. 949-954, September 18-21, 2001.

[2]. Cananau N., Ivanescu A., *Technological method of forestall of the superficial cracks network to the continuous cast slabs*, 1st International Conference on Advances in Materials and Processing Technologies, Leganes, Madrid, Spain, vol. 2, p. 955-960, September 18-21, 2001.

[3]. Anon, *Thin hot strip using planetry mill*, Steel Time International, 33-5, Sept. 1995.

[4]. Cananau N., Ivanescu A., *Study on the deformation process at the semi-planetary rolling*, Acta Mechanica Slovaca, Kosice, nr. 3, 2001.

[5]. Marina V., *The principles of passing from the microscopic state to the macroscopic one*, Metallurgy and New Materials Researches, vol. IV, nr. 2, p. 16-24, 1998.

[6]. Constantinescu S., *Mechanical properties of TiN thin films investigates using micromachining techniques*, METAL 2010, Ostrava, Czech Republic, ISBN: 978-80-87294-17-8, p. 926-931, 2010.

[7]. Constantinescu S., *Influence of heat treatment technology on the structure and properties of thin sheet steel ASTMS 14-degree F*, The Annals of "Dunarea de Jos" University of Galati, Fascicle IX Metallurgy and Materials Science, no. 1, p. 5-9, ISSN 1453-083X, 2015.

[8]. Constantinescu S., *Flat surfaces to obtain high quality products*, Journal TEHNOMUS - New Technologies and Products in Machine Manufacturing Technologies, ISSN-1224-029X, no. 20, p. 96-101, 2013.

THE ANNALS OF "DUNAREA DE JOS" UNIVERSITY OF GALATI.
FASCICLE IX, METALLURGY AND MATERIALS SCIENCE
N°. 2 - 2018, ISSN 1453-083X

MATHEMATICAL MODEL FOR THE OPTIMIZATION OF PREPARATION AND DELIVERY FLOWS AT LBC ADJUSTMENT

Marian-Iulian NEACȘU
"Dunarea de Jos" University of Galati, Faculty of Engineering, Romania
e-mail: uscaeni@yahoo.com

ABSTRACT

In the paper, the mathematical model of the sheet metal rolls handling process was realized in the LBC Adjustment section of Arcelor Mittal S.A. Galati. Mathematical modeling is performed by statistical methods, namely active regression analysis.

The modeling methods by experiment programming are very different because metallurgical processes are varied and complex.

We considered as the main influencing factors (the independent variables) the following parameters of the studied process:

1 - the number of rolls - n (number of rolled steel strips / entered in the section for 8 hours);

2 - the number of cranes - m (number of cranes / conveyor bridges from the LBC fitting section).

For the problem to be solved, the optimized function must have a physical meaning, be numerically expressed and show extreme values.

The objective function for optimizing the flow of rolled steel strips preparation and delivery from the LBC Adjustment section is represented by the storage space with some restrictions.

The best value for the objective function is found out by determining some values for the independent process variables, for which the conditions for obtaining some values imposed on dependent variables on minimum energy consumption Q are met.

KEYWORDS: mathematical modeling, optimization, rolls, storage space

1. Introduction

A basic tool useful both in the conception phase and in the analysis of the processes and operation of the installations is modeling. Determining the optimum for a metallurgical process is the result of combining mathematical modeling with the use of computers by using specialized programs [1].

The development of the specific mathematical apparatus and of the statistical methods has enabled the optimal decision-making issue to be tackled on the one hand as a problem of technical efficiency and, on the other hand, as a problem of high economic efficiency [2].

Mathematical models can be used to reveal optimal conditions, and as an important source of information necessary for optimal management of metallurgical processes [3].

This paper aims to combine the practice of optimization of metallurgical processes with the general techniques for solving extreme problems. All stages of an optimization calculation, from problem formulation to surface response research, are performed to determine optimal conditions in multifactor space [3].

The statistical methods for mathematical modeling suffer two important stages: the first stage, called the preliminary experiment, solves a series of problems mainly related to the selection of process factors and the interactions that may occur, the second stage called the experiment where the model is the real modeling and the statistical analysis of the model [4].

The variation of process factors is appreciated in the preliminary experiment by performing a series of program-based determinations (dispersion analysis, correlation analysis, etc.) that allows the selection of factors that significantly influence and highlights the

links between the factors and their contribution to the process [3].

2. Elaboration of the mathematical model of the sheet metal roll handling process in the LBC Adjustment section of Arcelor Mittal S.A. Galati

By using the active experiment, statistical methods are used at all stages of experimental research:

• before the experiment, by determining the number of experiences and the conditions for their realization;

• during the development of the experience by processing the obtained results;

• after the experiment ends with conclusions about future experiences.

The wording of the problem is the first step in solving it. Therefore, there needs to be a precise and clear formulation of the purpose of the work. For the problem to be solved, the optimized function must have a physical meaning, be numerically expressed and show extreme values [4].

Determining factors of influence i.e. independent variables is of great importance in solving optimization problems with experiment programming. Determining the optimal conditions may lose its meaning if one of the factors whose influence on the optimization parameter can be determined is neglected [3].

We considered the main factors influencing (the independent variables) the following parameters of the studied process:

1 - the number of rolls - n (number of rolled steel strips / entered in the section for 8 hours);

2 - the number of cranes - m (number of cranes / conveyor bridges from the LBC fitting section).

Table 1 shows the correspondence between the different levels of the factors expressed in natural values with those expressed in coded values for the two factors used in the studied process.

Table 1. *Correspondence between factor values expressed in natural units and coded units*

Factor	Number of rolls		Number of cranes	
	Natural units, in no. of rolls	**Stock coded**	**Natural units, in no. of cranes**	**Coded values**
Base level	n = 65	$\frac{65-65}{5}=0$	m = 2	$2-2=0$
Interval of variation	$\Delta u_1 = 40$	0	$\Delta u_2 = 8$	0
Higher level	n = 70	$\frac{70-65}{5}=+1$	m = 3	3-2 =1
Lower level	n = 60	$\frac{60-65}{5}=-1$	m = 1	1-2 = -1

For the coded representation of the experiment, the following notations and symbols were used:

Independent variables:

• x_1 - the number of rolls for delivery;

• x_2 - the number of cranes;

Between the natural and the coded values of the factors xi, the following relations exist:

$$x_1 = \frac{n-65}{5}; \quad x_2 = m-2; \qquad (1)$$

Yi values are expressed in natural units. The Yi values for the studied process represent the area occupied by the n rolls in the LBC Adjustment section.

Since the influence of the two factors on the performance of the process (Y) is studied, the experimental matrix shown in Table 2 was performed.

Further, based on the matrix of the complete factorial experiment, the coefficients of the regression equation (the mathematical model) are calculated.

Considering the function Yi as the analytical expression of the first order model, it is of the form [4]:

$$Y_i = c_0 + \sum_{i=1}^{3} c_i \cdot x_i + \sum_{\substack{i=1 \\ j=1 \\ i \neq j}}^{3} c_{ij} x_i x_j \qquad (2)$$

Table 2. *Experimental matrix of space occupied by rolls*

Nr. Exp.	x_0	x_1	x_2	x_{12}	Y
1	1	1	1	1	191
2	1	1	-1	-1	178
3	1	-1	1	-1	163
4	1	-1	-1	1	136

Equation (2) is written in matrix form as follows:

$$Y = X \cdot C \qquad (3)$$

where: X is the matrix of experimental condition.

$$X = \begin{Vmatrix} x_{01} & x_{11} & x_{21} & \dots & x_{m1} \\ x_{02} & x_{12} & x_{22} & \dots & x_{m2} \\ x_{03} & x_{13} & x_{23} & \dots & x_{m3} \\ \dots & \dots & \dots & \dots & \dots \\ x_{0n} & x_{1n} & x_{2n} & \dots & x_{mn} \end{Vmatrix} \qquad (4)$$

n- the number of rolls;
m- number of cranes;
C - the column vector of coefficients ci;
$C = [c_0, c_1, ..., c_n]^T$;
T - the symbol of matrix transposition;
Y - the experimental results matrix.

$$Y = [Y_1, Y_2, ..., Y_n]^T \qquad (5)$$

wherein: Y = [191, 178, 163, 136]

For the experiments performed, the matrix of the experimental conditions at the upper, lower and the basic level has the following form:

$$X = \begin{bmatrix} 1 & 1 & 1 & 1 \\ 1 & 1 & -1 & -1 \\ 1 & -1 & 1 & -1 \\ 1 & -1 & -1 & 1 \end{bmatrix} \qquad (6)$$

For this case, the linear function (6) has the form:

$$Y = b_0 + b_1 \cdot x_1 + b_2 \cdot x_2 + b_{12} \cdot x_1 \cdot x_2 \qquad (7)$$

Multiplying both terms of the matrix equation with the unit matrix to the left

E = [XT X] -1 × XT, resulting:
C = [XT × X] -1 [XT · Y] (8)

expression representing the relation of computation of the coefficients of the regression equation.

Using the values in Table 2, based on the relation (8), we obtain the coefficients of the order I, presented centrally in Table 3.

Table 3. *Coefficient values of the first order models*

Y_i / c_i	Y
b_0	668
b_1	70
b_2	44
b_{12}	-14

Therefore, the equation of the first order mathematical model (8) has the form:

$$Y = 668 + 70x\_1 + 44x\_2 - 14x\_1\ x\_2 \qquad (9)$$

By replacing the variables xi with the relations (1) in the equation above we obtain the following equation:

$$Y = -694 + 12.6 \cdot n + 200 \cdot m - 2.8 \cdot n \cdot m \qquad (10)$$

Interpreting the equation (10) shows that the greatest influence on the space occupied by the rolls is exercised by the number of cranes.

The next factor as weight of influence is the number of rolls received from the LBC.

Table 4 presents the values measured and estimated by calculation, using the equation of the mathematical model (10), as well as the data necessary to verify the suitability of the model by calculation.

Following calculations to verify the suitability of the model using the Fischer criterion method as well as the significance of the coefficients, it resulted that the first order mathematical model determined corresponds to the experimental data and can be used in the optimization of the sheet metal roll handling

process in the Arcellor LBC Adjustment section Mittal SA Galaţi with minimal costs.

Using the MATLAB version 2016 [5] software and based on the mathematical model obtained, a graphical interface for simulation of the surface occupied by sheet metal rolls was created in the LBC Adjustment section. Figure 1 and Figure 2 show a situation where a simulation of the surface occupied by sheet metal rolls is performed in the LBC Adjustment section.

Figure 1 shows the area covered by rolls ready for delivery when all three conveyors have worked for 8 hours. Figure 2 shows the simulation of the situation when only two conveyors are available during the 8 hours of operation.

Table 4. *Table of measured and calculated values for Y*

Nr. crt.	$Y_{1\ measured}$ m^2	$Y_{1\ Calculated}$ m^2	$Y_{1\ measured} - Y_{1\ Calculated}$ m^2	$(Y_{1măs} - Y_{1calc})^2$ m^2
1	191	195	4	16
2	178	182	-4	16
3	163	158	5	25
4	136	120	16	256

Fig. 1. *Simulation of the area occupied by rolls in the LBC Adjustment section when all three conveyors have worked for 8 hours*

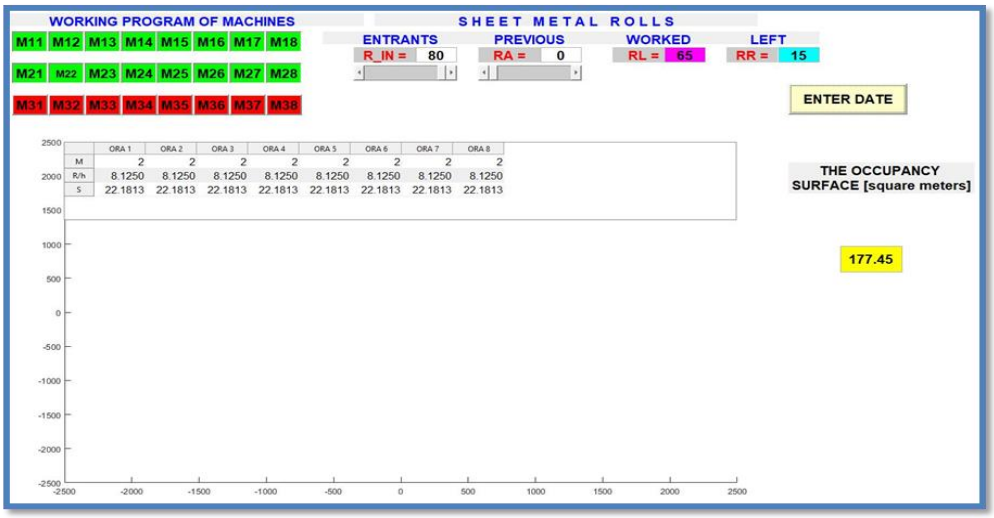

Fig. 2. *Simulation of the area occupied by rolls in the LBC Adjustment section when only two out of the three conveyors have worked for 8 hours*

3. Conclusion

In this paper was achieved the mathematical model of the sheet metal roll handling process in the LBC Adjustment section of Arcelor Mittal S.A. Galati. Mathematical modeling was performed by statistical methods, namely regression analysis by active experiment.

Analyzing the influence of each parameter on the analyzed process, based on the final form of the mathematical model we can say that:

• the greatest influence on the analyzed process is exercised by the term (parameter m) whose coefficient has the highest positive value. This is the number of cranes available.

• the second parameter of the process, namely the number of rolls, has a smaller influence on the process finality because it has a positive coefficient, but which is lower than the other parameter

When the parameter, the number of cranes has a maximum value (m = 3), the area occupied by the number of rolls ready for delivery will be directly proportional to the number of maximum rolls received or entered the process.

When the parameter, the number of rolls has a maximum value (n = 70), the area occupied by the number of rolls is directly proportional to the maximum number of functional cranes in an 8h shift.

The values calculated for the optimized parameter using the mathematical model developed (Y) are very close to the measured values, so the mathematical model presented allows the simulation of the preparation and delivery process rolls at the LBC Adjustment.

Based on the obtained mathematical model, two prediction programs (simulation) of the surface occupied by rollers in the LBC Adjustment section were made using MATLAB software.

References

[1]. Ciucă I., Dumitriu S., *Modelarea şi Optimizarea Proceselor Metalurgice de Deformare Plastică şi Tratamente Termice*, Editura Didactică şi Pedagogică, Bucureşti, 1998.

[2]. Popescu D., Ionescu F., Dobrescu R., Ştefanoiu D., *Modelare în ingineria proceselor industriale*, Editura AGIR, Bucuresti 2011.

[3]. Taloi D., *et al.*, *Optimizarea proceselor metalurgice*, Editura Didactică şi Pedagogică, Bucureşti, 1983.

[4]. Taloi D., *Optimizarea proceselor tehnologice – aplicaţii în metalurgie*, Editura Academiei, Bucureşti, 1987.

[5]. Ghinea M., Fireţeanu V., *MATLAB – calcul numeric – grafică – aplicaţii*, Editura Teora, ISBN 973-601-275-1, Bucureşti, 1998.

[6]. Baron T., *et al.*, *Statistică teoretică şi economică*, Editura Didactică şi Pedagogică. Bucureşti, 1995.

THE ANNALS OF "DUNAREA DE JOS" UNIVERSITY OF GALATI.
FASCICLE IX, METALLURGY AND MATERIALS SCIENCE
N°. 2 - 2018, ISSN 1453-083X

USE OF BIODEGRADABLE SORBENTS TO THE DECONTAMINATION OF POLLUTED SOILS

Lucica BALINT
"Dunarea de Jos" University of Galati, Faculty of Engineering, Romania
e-mail: lbalint@ugal.ro

ABSTRACT

The paper presents the decontamination of soils polluted with diesel, oils and other petroleum products. Soil decontamination is applied in-situ and ex-situ, depending on the surface and depth of the polluted area. The treatment time was 152 days, after which total hydrocarbon oil concentrations decreased for all experimental samples. The highest efficiency in reducing the concentration of petroleum products was in the case of samples treated with biodegradable sorbent and in the case of those treated with biodegradable sorbent mixture and biological sludge. Biodegradable non-waste materials have been used. The risk of migration of deep pollutants is low in the ex-situ version. Decontamination time is longer for high yields. In the case of older pollution, decontamination yields are low due to the presence of some 35% compounds, which do not migrate and are difficult to biodegrade under normal conditions.

KEYWORDS: decontamination, biodegradable sorbent, polluted soils

1. Introduction

Based on data provided by the national soil quality monitoring system, it is estimated that 900,000 ha of soil are chemically polluted, of which 200,000 ha are excessively polluted, making them completely unproductive. On an area of 50,000 ha the soils in Romania are polluted with petroleum products; although the affected area has decreased in recent years, pollution continues to have a significant impact on the soil. Approx. 3,000 ha are completely removed from plant production, especially around oil exploration wells and along oil pipelines (in the counties of Prahova, Teleorman, Braila, Galati, Arges, Dambovita). The extraction of salt through the wells caused intense soil pollution on tens of hectares, with brine and oil products. Pollution of heavy metals and sulfur dioxide is identified especially in Baia Mare, Zlatna, Copsa Mica. To this was added the pollution with domestic and industrial residues. Soil irrigation in some rivers (Olt, Argeș, Mureș, Prahova, Siret), where toxic substances and oil products are discharged, leads to the progressive accumulation of pollutants in the soil, with serious consequences for human health.

The particular aspect of soil and groundwater pollution with crude oil and petroleum products for Romania is that it is a phenomenon with a history of more than 100 years, which started with the beginning of the exploitation of the oil deposits in the Prahova valley area and with the emergence and development petroleum industry.

In the field of ecological reconstruction of soils, measures were taken consisting of:

• inventorying contaminated, degraded land and other deficiencies;

• substantiating recommendations for good agricultural practices aimed at preserving and improving the quality of agricultural soils in line with international practices;

• substantiating ecological reconstruction measures for soils polluted with heavy metals;

• the scientific foundation of re-cultivation of mining waste dumps;

• leading experiments on the detoxification of soils polluted with crude oil, products and petroleum residues through bioremediation;

• performing technical and scientific substantiation of the polluting of polluted soils with mineral oils and polychlorinated biphenyls (PCBs) from Transelectrica S.A. [1].

Decontamination by sorbents is done by spreading them on the polluted surface, ensuring optimal contact between pollutant and sorbent. In some cases, bioremediation accelerators (strains of bacteria and/or fungi) are used, as well as the application of soil improvement treatments by

providing the aerobic conditions, ensuring the necessary humidity and restoring nutrient balance by fertilization.

Contaminated soil portions are in the vicinity of fuel depots, oil discharge areas, wagon repair areas, and railroad tracks. In accordance with the MAPPM Order no. 756/1997 for the approval of the Regulation on the assessment of environmental pollution, the reference values for traces of chemical elements in soils for oil hydrocarbons are presented in Table 1 [2, 3].

Table 1. *The reference values for traces of chemical elements in soils from petroleum hydrocarbon (mg/kg dry matter)*

Traces of pollutant	Normal values	Alert Thresholds / Types of Usage		Intervention Thresholds / Types of Usage	
		Sensitive	Less sensitive	Sensitive	Less sensitive
TPH (Total Petroleum Hydrocarbon)	< 100	200	1000	500	2000

2. Experiments and discussions

Biodegradable non-waste materials are used. Contaminated soil samples were taken which were treated with: a) NatureSorb type biodegradable sorbent; b) biodegradable mixture; c) biological sludge, respectively beech sawdust. The monitoring of the biodegradation process was carried out by periodic analyses of the quality indicators.

Sampling of soil samples was carried out in accordance with STAS 7184 / 1-1984 and Order no. 184/1997 of MAPPM. The soil samples were taken at two depths of 5 cm and 30 cm respectively [2, 4].

The number of samples taken was after the contaminated areas, 14 soil samples and two control samples.

For the collected soil samples the quality indicators were determined: pH, Humidity, Humus, Total Organic Carbon (TOC), Total Kjeldhal Nitrogen (NTK), Total Phosphorus and Total Petroleum Hydrocarbon (TPH) with the methods of analysis provided by the actual standards.

Following the laboratory analyses for soil samples, the values of the quality indicators presented in Table 2 were obtained.

Table 2. *Quality indicators of selected samples before treatment*

Nr. crt.	Sample code	Depth of sampling, [cm]	pH	TPH, [mg/kg d.m.]	TOC, [% d.m.]	NTK, [% d.m.]	P total, [mg/kg d.m.]
1.	Pm1	5	7.08	1859.12	1.25	0.142	0.073
2.	Pm2	30	7.14	1738.23	1.18	0.154	0.081
3.	Pm3	5	6.85	2147.34	1.82	0.098	0.085
4.	Pm4	30	6.94	1973.11	1.67	0.109	0.074

Each soil sample had 0.5 kg. Sample labelling was the following: 1) witness samples: Pm1, Pm2, Pm3, Pm4; 2) samples treated with NatureSorb biodegradable sorbent: Ps1, Ps2, Ps3, Ps4; 3) samples treated with sorbent mixture and biological sludge: Pss1, Pss2, Pss3, Pss4; 4) sorbent-treated samples of beech sawdust natural type cu: Psb1, Psb2, Psb3, Psb4.

The biodegradable sorbent was added in the ratio: concentration petroleum products / sorbent was 1: 3. To the samples labelled with „ss" was added 900 mL / biological sludge sample. The biological sludge used was taken from the recirculation system of a water treatment plant. In samples labelled with "sb", sawdust was added in the ratio: concentration petroleum / sawdust was 1:5. Ambient temperature was maintained between 21-35 °C to ensure optimal microorganism development and fluidity of petroleum products, and soil moisture was between 20-40% to favour absorption processes. No additional amounts of nutrients (nitrogen, phosphorus, etc.) were added, and sample aeration was done 3-4 days [5, 6].

The values for total petroleum hydrocarbons obtained are shown in Figures 1-3.

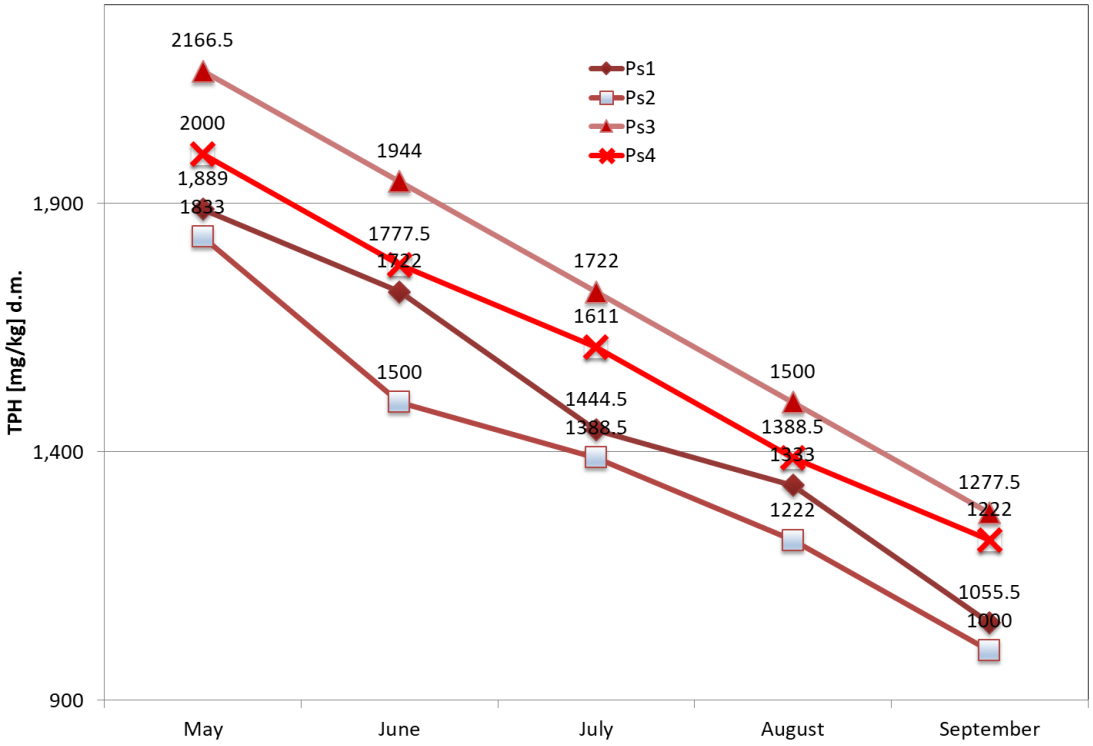

Fig. 1. *Variation of total petroleum hydrocarbon for samples treated with biodegradable sorbent*

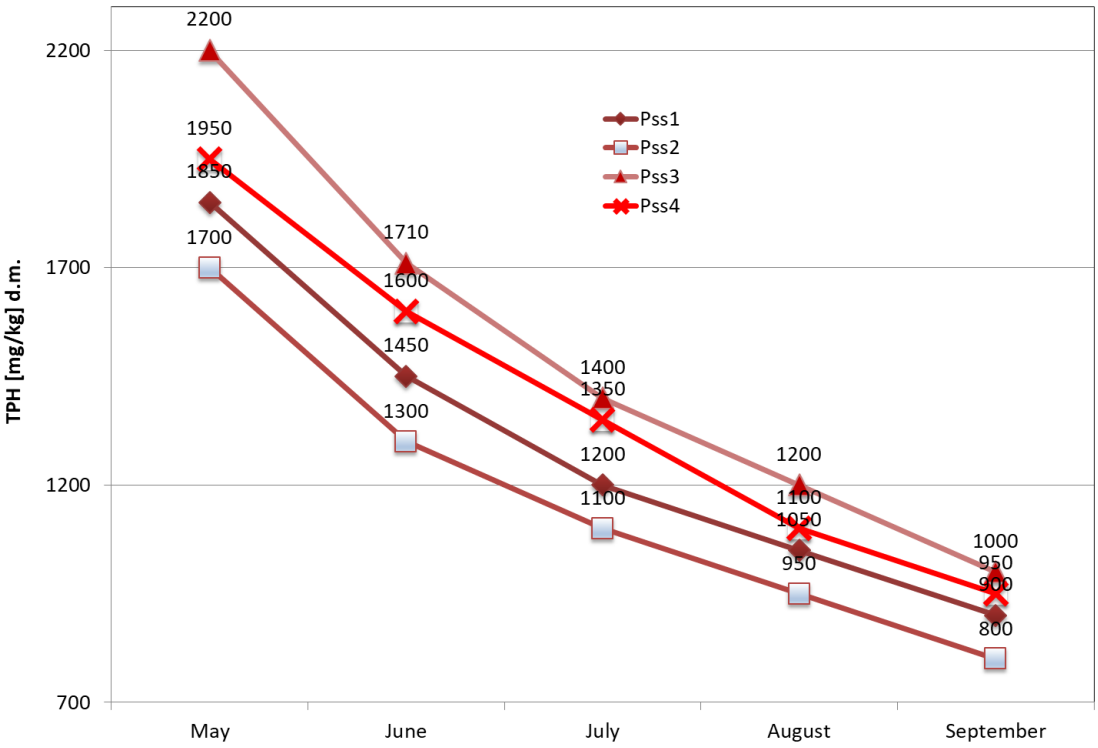

Fig. 2. *Variation of total petroleum hydrocarbon for samples treated with sorbent mixture and biological sludge*

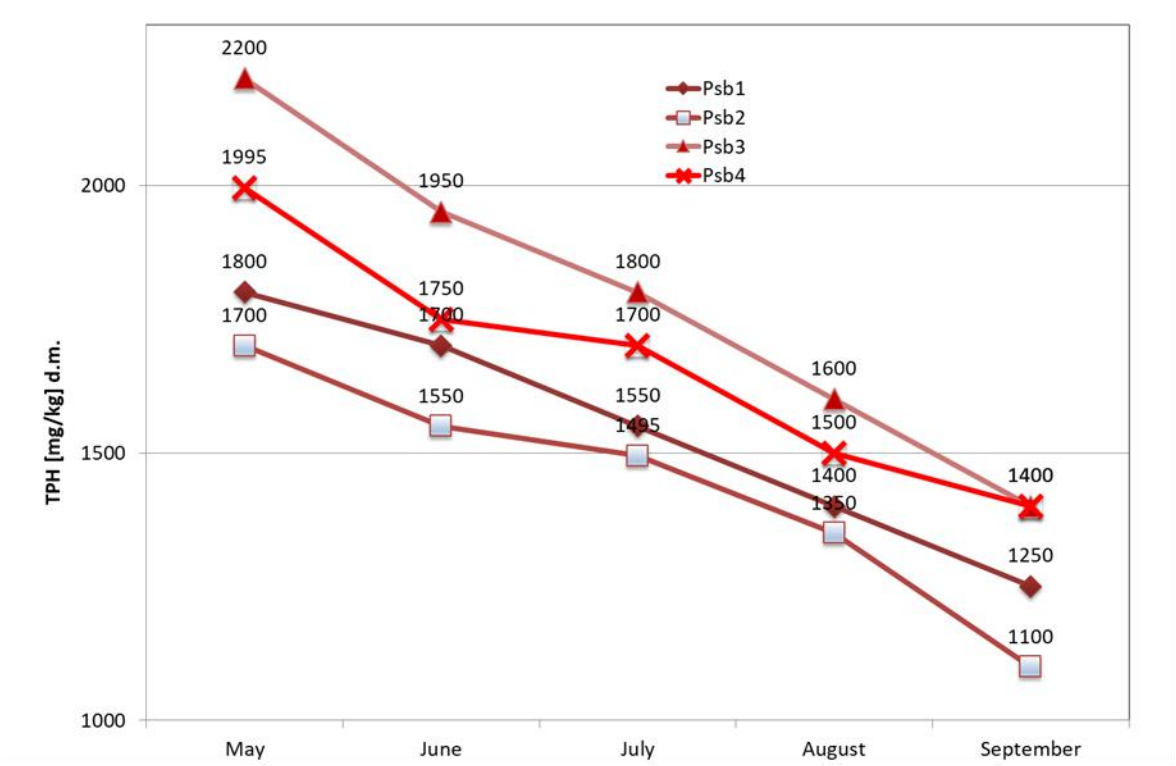

Fig. 3. *Variation of total petroleum hydrocarbon for samples treated with beech sawdust*

Following the analysis of the results obtained were ascertained the following:

a) the TPH values in the analysed samples exceeded the alert threshold of 1000 mg/kg d.m. for samples with code P1, P2, P4 as well as the intervention threshold of 2000 mg/kg d.m. for sample P3;

b) the gas chromatography mass spectrometry (GC/MS) analysis demonstrated that significant concentrations of diesel (C8-C22) and mineral oils (C20-C40), is relatively stable fractions, which migrate less in the soil, both horizontally and vertically;

c) pH values are within normal, neutral to slightly alkaline ranges, between 6.5 and 8.5;

d) the percentage of humus in the analysed samples indicates a low and medium supply, and the amount of nitrogen and phosphorus present in the samples is very low, indicating a very low nutritional intake [7, 8].

For samples with high initial concentrations of total oil in oil, P3 and P4, concentrations below the alert threshold required by the legislation were recorded only when treated with a mixture of sorbent and biological sludge.

Values of decontamination yields obtained for P3 and P4 samples are shown in Figures 4-5.

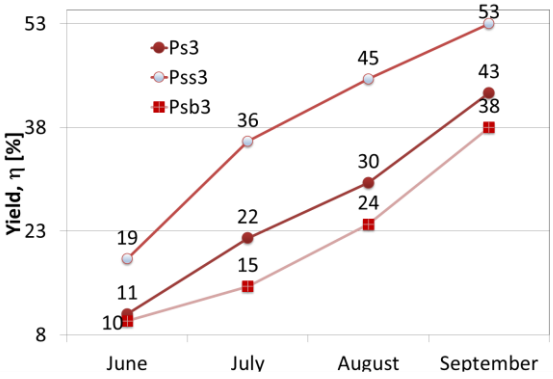

Fig. 4. *Decontamination yields for P3 samples*

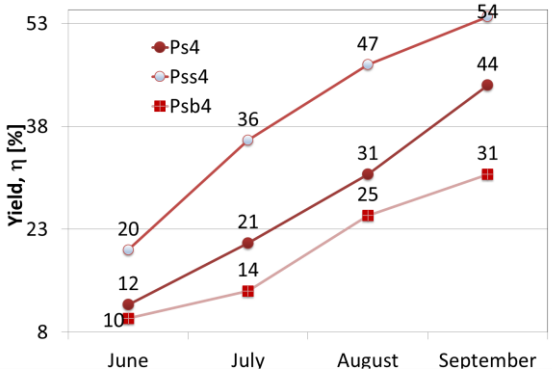

Fig. 5. *Decontamination yields for P4 samples*

3. Conclusions

After 153 days of treatment, total hydrocarbon oil concentrations showed a decrease for all experimental samples.

For sample Ps2 with large initial concentrations of total hydrocarbon oil, decreases in concentrations below the alert threshold required by the legislation were only observed when treated with biodegradable sorbent.

The highest efficiency of reducing the concentration of petroleum products was recorded for samples treated with biodegradable sorbent mixture and biological sludge Pss1, Pss2, Pss3, Pss4.

The decontamination yields showed a steady increase during the experiments, with the best yields being obtained for the samples added to the biodegradable sorbent and biological sludge with a maximum of 54%.

Satisfactory decontamination yields are also obtained for samples treated with biodegradable sorbent only, with values ranging from 43-44%.

The pollutant migration risk is low in the ex-situ version.

Decontamination time is long to get good returns.

References

[1]. Neag Gh., *Decontamination of soils and groundwater*, House of Science Book Publishing House, Cluj, 1997.
[2]. ***, *Order no. 756/1997 of MAPPM for the approval of the Regulation on the assessment of environmental pollution*.
[3]. ***, *Catalog of Romanian Standards*, 2007.
[4]. ***, *Methods of chemical soil analysis*, Research Institute for Pedology and Agrochemistry, Bucharest, 1986.
[5]. Stroud J. L., Paton G. I., Semple K. T., *Microbe-aliphatic hydrocarbon interactions in soil: implications for biodegradation and bioremediation*, Journal of Applied Microbiology, UK, vol. 102, May 2007.
[6]. Chaerun Siti Khodijah, Asada Ryuji, Tazaki Kazue, *Biodegradation of heavy oil from the Nakhodka oil spill by indigenous microbial consortia*, International Journal of Applied Environmental Sciences, June 2007.
[7]. Jirasripongpun K., *The characterization of oil-degrading microorganisms from lubricating oil contaminated soil*, Journal of Applied Microbiology, UK, vol. 35, October 2002.
[8]. ***, http://www.ecologic.rec.ro/articol/read/stiinta-tehnologie/2138.

THE ANNALS OF "DUNAREA DE JOS" UNIVERSITY OF GALATI.
FASCICLE IX, METALLURGY AND MATERIALS SCIENCE
N°. 2 - 2018, ISSN 1453-083X

WASTEWATER TREATMENT CASE STUDY - SEAU BRĂILA

Lucica BALINT
"Dunarea de Jos" University of Galati, Faculty of Engineering, Romania
e-mail: lbalint@ugal.ro

ABSTRACT

The paper analyses the influent and effluent parameters, as well as the efficiency of the purification process. CBO_5 is found to be within the legal limits in terms of the amount of effluent suspensions of max 6.0 mg/L O_2. The efficiency of their removal from the influent was at least 94.8%. CCO is observed within the legal limits of the amount of effluent suspensions of max 20.2 mg/L O_2. The efficiency of their removal from the influent was at least 93.0%. Suspended matter shows that the effluent sludge was within the legal limits of max 10.9 mg/L, and the efficiency of their removal from the influent was at least 91.6%. Total nitrogen (N_{total}) and total phosphorus (P_{total}) are exceedances of the limits for sensitive areas subject to eutrophication. A downstream denitrification step is proposed downstream of the aerobic stage to eliminate total nitrogen, and a phase of chemical treatment or alternation of aerobic and anoxic steps is proposed for the removal of total phosphorus.

KEYWORDS: water treatment, wastewater, influent, effluent

1. Introduction

The current period is experiencing an accelerated development of urban settlements and especially of metropolises. Centralized water and wastewater/municipal water treatment systems are being developed and modernized in an accelerated manner. The systems cover distances of tens, hundreds of kilometers, serve tens of thousands, hundreds of thousands of inhabitants and operate 24 hours a day, provide wastewater treatment with increasingly complex techniques to meet quality standards.

Treatment technologies consist of processes or operations designed to reduce pollutants in wastewater to an acceptable level depending on the effluent destination.

Analyzes are performed by in-situ sensors in the laboratory to obtain data on the operation of a wastewater treatment plant in a timely manner with the possibility of rapid intervention of parameter adjustments and of historical trend setting.

Production reports based on these data are the source of the data needed to investigate the relationship between the input and output parameters of a wastewater treatment plants.

Effective treatment technology is a combination of processes or operations designed to reduce certain constituents in wastewater (reducing or removing organic, solid, nutrient, metals, microorganisms or other pollutants) to an acceptable level depending on the effluent destination. The purpose of wastewater treatment is to enable safe disposal of these waters without endangering public health and not pollute surface water, groundwater, or pollute the environment. a) Preliminary treatment aims to prevent damage in later stages of treatment as a result of the presence in the water of substances at concentrations and characteristics that do not allow the optimal development of physical, chemical or biological processes specific to the treatment technology. b) Primary treatment may be based on physical processes-based operations such as sedimentation, flotation and decantation. c) Secondary treatment is based on the decomposition of dissolved or colloidal organic matter in the decanted water by means of microorganisms. Secondary treatment can be done in one step at small organic loads or in two steps at high organic loads. d) Tertiary treatment will allow the elimination of non-biodegradable organic and mineral substances by filtration in granular media and generally applies to industrial wastewater. Dephosphating and denitrification are specific tertiary treatment operations that apply to wastewater treatment plants. e) In advanced treatment, residual solid suspensions and other wastewater constituents that could not be reduced by previous treatments are removed by

combined application of unitary processes (reverse osmosis, electrodialysis, selective ion exchange, oxidation, detoxification, etc.) [1, 2].

2. Research and results

At the treatment plant, the influent and effluent parameters are followed, as well as the efficiency of the purification process to regulate the process. The most important data are given in Table 1 and Table 2.

Table 1. *Influent / effluent monthly averages of parameters: temperature, pH, solids in suspension (SS), NH_4^+, NO_3^-*

Month	Temp. [°C]		pH		SS [mg/L]			NH_4 [mg/L]			NO_3 [mg/L]	
	Influent	Effluent	Influent	Effluent	Influent	Effluent	Efficiency	Influent	Effluent	Efficiency	Influent	Effluent
June	21.7	21.8	7.8	7.9	144.6	10.3	92.5	40.9	9.5	75.2	2.1	31.4
July	25.8	25.9	7.8	8.0	193.7	10.1	94.2	44.6	1.0	98.6	3.3	44.5
August	25.7	25.8	7.7	7.9	225.1	9.3	95.5	51.4	2.3	97.5	2.2	37.5
September	23.4	23.4	7.7	7.9	171.2	6.7	96.1	63.0	3.1	92.3	8.4	52.9
October	21.1	20.6	7.6	7.6	265.5	10.9	95.7	58.1	1.5	95.5	3.4	47.5
November	17.3	17.1	7.5	7.4	213.5	8.1	96.0	50.2	1.2	97.8	2.5	57.4
December	11.9	11.5	7.6	7.4	131.2	10.2	91.6	51.8	3.1	94.1	4.3	42.7

Table 2. *Monthly Influence / Influence Parameter Mediums: CBO_5, CCO-Cr, N_{total}, P_{total}*

Month	CBO5 [mgO_2/L]			CCO-Cr [mgO2/L]			Ntotal [mg/L]			Ptotal [mg/L]		
	Influent	Effluent	Efficiency	Influent	Effluent	Efficiency	Influent	Effluent	Efficiency	Influent	Effluent	Efficienta
June	172.2	8.1	94.8	353.5	20.3	94.1	48.5	13.7	71.7	7.9	4.2	45.6
July	187.9	8.6	95.2	379.7	24.4	93.1	41.8	13.2	67.9	4.9	1.8	63.2
August	215.9	8.7	95.6	458.3	24.7	94.1	41.9	14.9	68.7	4.6	1.6	67.2
September	173.3	7.6	95.6	384.1	21.6	94.3	43.1	13.0	69.8	5.5	2.9	41.8
October	222.3	6.4	96.9	504.6	21.2	95.6	45.7	12.8	71.9	5.3	0.6	95.6
November	207.9	6.0	96.9	454.5	22.1	95.0	71.6	20.9	70.9	3.9	1.9	51.2
December	174.5	6.0	96.3	334.9	22.7	93.0	42.5	13.0	65.7	3.1	1.7	52.2

Concerning the suspended materials, a compliance with the legal limits is observed both in terms of the amount of effluent suspensions (< 40 mg/L) and the effluent removal efficiency (> 90%).

Regarding N_{total}, there are exceedances of the legal limits in the effluent (> 10 mg/L) and there is a low efficiency of its elimination from the influent. This can be corrected by future investments in the new capacity of the station. A de-nitrification step downstream of the aerobic stage can be achieved.

Regarding P_{total}, there are exceedances of the legal limits in the effluent (> 1%) and there is a low efficiency of its elimination from the influent. In this field, corrections can also be made through investments that may involve a chemical treatment or the successive alternation of aerobic and anoxic steps [3, 4].

It is a direct relationship between the evolution of the efficiency of the elimination of the chemical oxygen consumption and the efficiency of the elimination of the biochemical oxygen consumption. This is shown in Figure 1, in which variation of elimination efficiency of NH_4^+, CBO_5, CCO-Cr was represented in June-November. In June, due to a deficiency due to nonlinearities in the operation of the aeration system, there is a decrease in the efficiency of ammonium elimination in wastewater.

In aeration basin, where nitrification is carried out in an O_2-enriched environment, metabolic processes of multiplying the microorganisms responsible for this process occur. This organic substance increases the amount of sludge. The variation of the sludge quantity and volatile matter quantity in the months of June-November is shown in Figure 2. For plotting the graph, we used the data corresponding to the aeration basin, which worked without stopping during the entire period [5, 6].

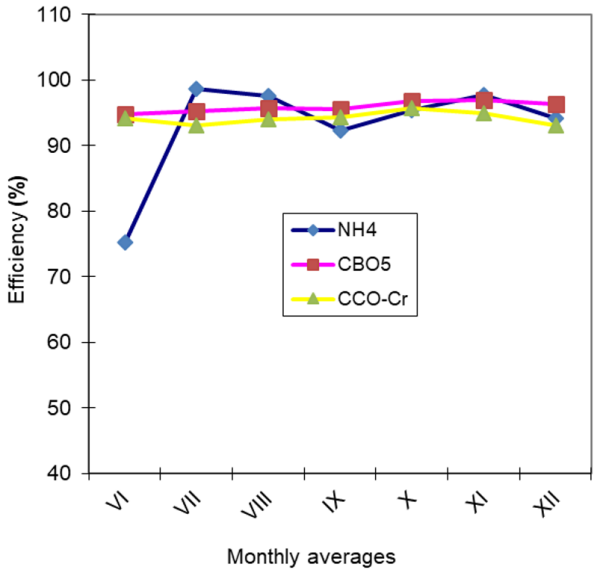

Fig. 1. *Variation of elimination efficiency of NH_4^+, CBO_5, CCO-Cr*

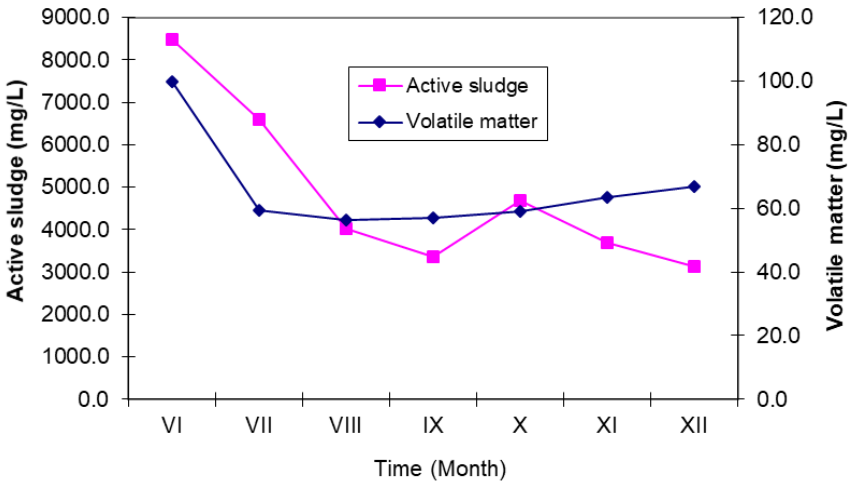

Fig. 2. *Variation of sludge and volatile content in the aeration tank in mg/L*

3. Conclusions

At SEAU Brăila, active sludge is used as the main treatment medium. The composition of wastewater determines both the size of the treatment plants and the quality of the surface water that may occur in the choice of process and treatment scheme.

At the base of the waste water treatment plant design, the current data on the equivalent population – 143,333, the CBO_5 load – 8,600 kg/day, the solid suspension load - 11,940 kg/day, and the forecast for 2026 (the equivalent population - 266,667, CBO_5 loading - 16,000 kg/day, solid loading suspension - 20,400 kg/day.

In the analysed period, the CBO_5 is within the legal limits both in terms of the amount of effluent suspensions of max 6 mg/L O_2 compared to the expected max. 25 mg/L O_2 and the efficiency of their elimination from the influent of 94.8% compared to 90% at least).

At CCO, a legal compliance is observed both in terms of the amount of effluent suspensions of max 20.2 mg/L O_2 compared to the maximum of 125 mg/L O_2 provided, as well as the efficiency of their elimination from with an influence of at least 93.0% compared to the expected 75%.

Suspended materials show compliance with the legal limits both in terms of the amount of effluent suspensions of max 10.9 mg/L compared to the predicted max. 35 mg/dm^3 and the efficiency of their elimination from the influence of minimum 91.6% versus at least 90% predicted.

At N_{total} and P_{total}, exceedances of the boundaries for sensitive areas subject to eutrophication are observed both in terms of the effluent concentration and the efficiency of its elimination from the influent. This deficiency can be corrected by a de-nitrification step downstream of the aerobic stage to eliminate N_{total}, and for P_{total} a chemical treatment step can be implemented, or successive alternating aerobic and anoxic steps can be employed.

References

[1]. Maria Vlad, *Course and laboratory notes for Water Management discipline*, 2011.
[2]. Lucica Balint, *Course and laboratory notes at the Cleaning and Wastewater Treatment Technologies discipline*, 2011.
[3]. Marian Petre s.a., *Original synthesis Course COPMED – POSDRU/81/3.2./S/52242-Tratarea şi epurarea apelor uzate*, 2012-2013.
[4]. ***, *H.G. 188/20.03.2000 for the Adoption of Standards for Discharge in the Aquatic Environment of Wastewater*, Modified and Completed by H.G. 352/11.05.2005.
[5]. Mihail Chiriță, *Waste Water Treatment Plant Brăila*, http://www.araromaqua.ro/index.php/arhiva - revista/49-2012/91-romaqua-numarul-1-2012, 2012.
[6]. Matei Doru, *Research on Urban Waste Water Treatment and Environmental Risk Assessment*, Dissertation 2013.

THE ANNALS OF "DUNAREA DE JOS" UNIVERSITY OF GALATI.
FASCICLE IX, METALLURGY AND MATERIALS SCIENCE
N°. 2 - 2018, ISSN 1453-083X

STUDIES AND RESEARCH ON WATER POLLUTION IN GALATI URBAN AREA

Stela CONSTANTINESCU
"Dunarea de Jos" University of Galati, Faculty of Engineering, Romania
e-mail: constantinescu_stela @ugal.ro

ABSTRACT

The purpose of the work was the study of wastewater treatment at the Galati sewage Station in June, August 2017 and January, February, April and May 2018. The treatability can be expressed by removing the total organic substances from water (determined by CCO or cot tests) or by removing equivalent substances (determined by the CBO test). The reduction of CCOCr and CBO_5 from wastewater after passing through the installation of the Galati treatment station is an estimate of the quantity of organic substances removed in the treatment process. As a result of the determination of the concentration of organic substances in the influence and effluent of the Galati treatment station, the following were found: The Symons environmental treatment ratio achieved for influence was 0.554 which framed the influence in S.E. Galati in the category of wastewater readily treatable by biological methods, in the presence of naturally occurring micro-organisms in these waters. Another criterion for assessing the treatability of wastewater is the efficiency of reducing CCOCr and CBO_5. The efficiency of reduction of CCOCr (81%) and CBO_5 (84%) allow for the characterization of wastewater as a biological treat in S.E. Galati and alongside the operation at optimum parameters of treatment plants.

KEYWORDS: water pollution, organic substances, efficiency of reducing CCOCr and CBO_5, characterization of wastewater

1. Introduction

The purpose of the work was the study of wastewater treatment at the Galati sewage Station in June-August 2017 and January-May 2018. To determine whether a wastewater is cleansed biological, the notion of treatability has been introduced. Treatability is the capacity of a wastewater to reduce its complexity and number of organic components due to the action of microorganisms present in wastewater treatment plants. This notion accumulates several factors, such as: the ability of organic constituents to be biodegraded; the ability of micro-organisms to degrade organic components; the time it takes to biodegradation organic components [1-3]. The treatability can be expressed by removing the total organic substances from water (determined by CCO or COT tests) or by removing equivalent substances (determined by the CBO test). The Galati treatment station receives and encloses about 3200 L/s wastewater from Galati, of which ~80% are household waters and ~20% are industrial wastewater and partly rainwater from most of the city's territory. Galati Treatment Station is an installation that comprises the stages of primary physico-mechanical treatment (gratings, fat separators, decanters) and biological secondary with active sludge [4-6].

2. Experimental conditions

In order to achieve the proposed purpose, samples of wastewater were collected from three harvest points, twice a week, during the periods of the year 2017 and 2018 respectively. The scheme of the treatment plant and the harvesting points are shown in Figure 1.

The daily average test of influence is made up of samples of 100 mL of time harvested through an automated device for 24 hours that have been homogenized. The EM sample represents a 12-hour average sample consisting of samples of 400 mL harvested every 2 hours that have been homogenized. The EB samples were harvested and processed similarly as EM. The daily harvest hours of the two effluents were: 7, 9, 11, 13, 15 and 17.

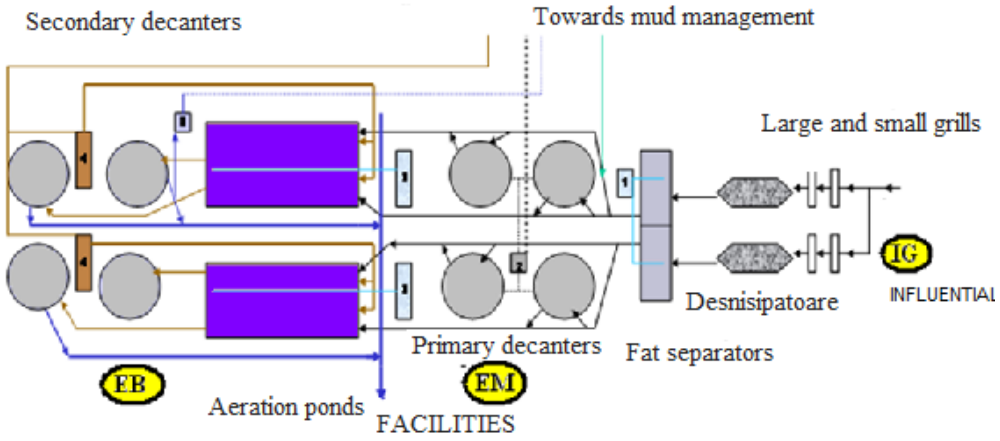

Fig. 1. *Diagram of the treatment plant Galati and sample sampling points: IG-General entry; EM – Mechanical step evacuation; EB – Removal of the biological step*

The samples analysed are representative samples for the collection points. Thus, the influence represents a 24-hour average sample, and effluents average samples for 12 hours. Considering that the average retention time of wastewater through wastewater treatment equipment is 8 hours, it can be considered that analyses carried out on the influence and effluent are appropriate. Following the quantitative determinations of the main parameters indicating the degree of pollution of the emissary with global organic material, the results have been synthesized and processed in order to determine important treatment indicators, such are the report of Symons treatability and treatment efficiency. The Symons treatability report expresses, indirectly, the ratio between the quantity of biodegradable substances and the quantity of oxidizable substances in the waters subject to pollution.

3. Results and discussions

The characterization of wastewater taken from each step of the technological process determined the content of organic materials by means of global parameters (CCOCr, CBO_5). The reduction efficiency of CCOCr and CBO_5 was also calculated. The obtained results were compared with the limits laid down in the legislation. The CBO_5 and CCOCr load limit values according to HG 352/2017 and the minimum reduction percentage are shown in Table 1.

The results obtained in the months, August 2017 and May 2018 are presented in Figures 2 to 3, 2017 and 4-5, 2018.

Table 1. *The CBO_5 and CCOCr load limit values according to HG 352/2017 and the minimum reduction per centage*

Parameters	**Concentration, mgO_2/L**		**Minimum discount percentage %**	**Reference method of measurement**
	Influent NTPA 002/2017	**Effluent NTPA 001/2017**		
CBO_5 la 20±1ºC no nitrification	300	25	70-90	Homogenized, unfultered sample, nolodged. Determination of the O_2 disolved before and after an incubation of 5 days at 20 ºC±1 ºC, in complete darkness. Addition of nitrification inhibitor.
CCOCr	500	125	75	Homogenized, unfultered sample, nolodged. Potassium dichromate.

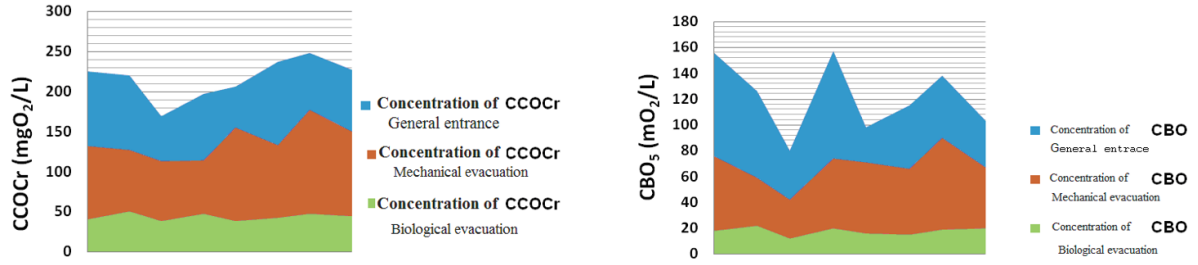

Fig. 2. *Dynamics of the evolution of CCOCr and CBO_5 concentrations month August 2017*

In August 2017 the average reduction efficiency of CCOCr was 36% at the mechanical stage, 69% at the biological stage and 80% total station.

In August 2017 the average reduction efficiency of CBO_5 was 44% at the mechanical stage, 74% at the biological stage and 86% total station.

In May 2018 the average reduction efficiency of CCOCr was 45% at the mechanical stage, 51% at the biological stage and 72% total station.

In May 2018 the average reduction efficiency of CBO_5 was 42% at the mechanical stage, 67% at the biological stage and 81% total station.

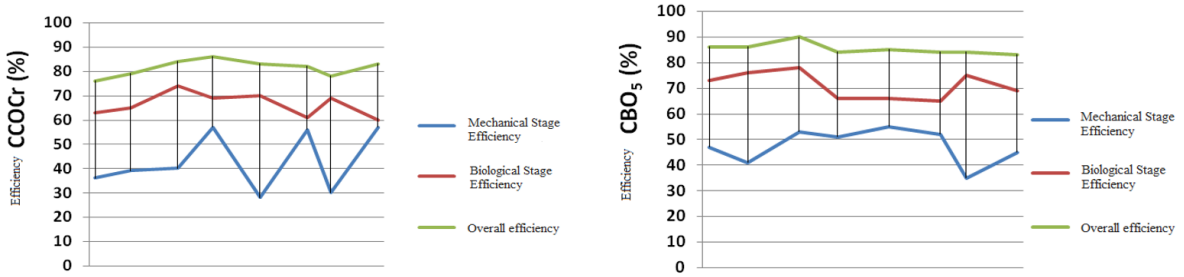

Fig. 3. *The dynamics of efficiency of reduction of CCOCr and CBO_5 in August 2017*

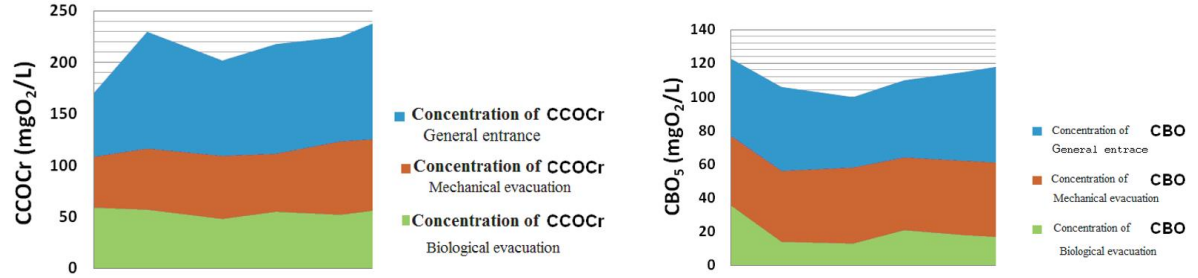

Fig. 4. *Dynamics of the evolution of CCOCr and CBO_5 concentrations in May 2018*

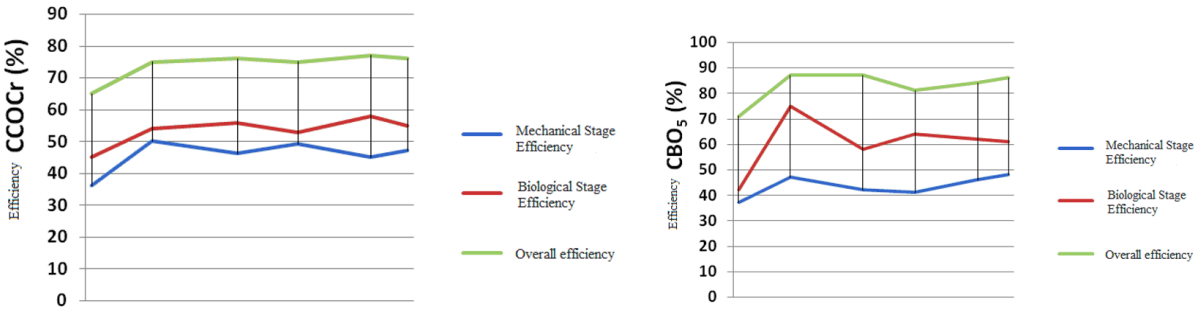

Fig. 5. *The dynamics of efficiency of reduction of CCOCr and CBO_5 in May 2018*

All concentrations recorded in CCOCr both in the influence and the effluent of Galati respected the limits permitted by the legislation in force (500 mgO_2/L in influence and 125 mgO_2/L in the effluent). As regards CBO5 it is observed that in influence and in effluent the concentration was within the permissible limit value (300 mgO_2/L) and (25 mgO_2/L) respectively.

The concentrations of the analysed parameters present homogeneous values in all the samples analysed.

In Figure 6 the dynamics of the average efficiency reduction of CCOCr and CBO_5 in mechanical, biological step compared to the general efficiency of the Galati station in 2017 and 2018 are presented.

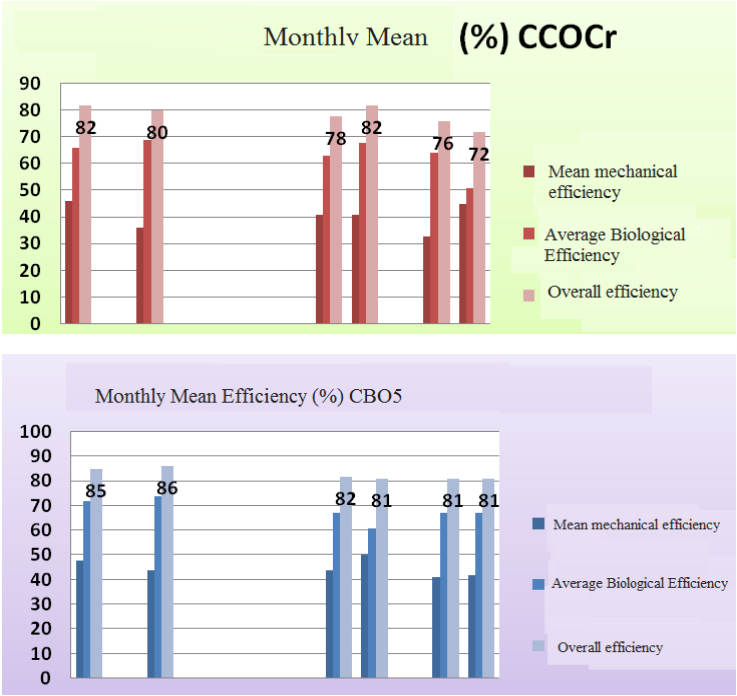

Fig. 6. *The dynamics of the average monthly reduction efficiency of CCOCr and CBO_5 in 2017 and 2018*

The average reduction efficiency of CCOCr falls between 36-46% for the mechanical step, with the average of 40%, and between 67-74% for the biological step, with the average of 64%. The average reduction efficiency of CBO_5 falls between 41-50% for the mechanical step, with the average of 45% and between 61-74% for the biological step, with the average of 68%.

The general reduction efficiency of the Galati treatment station is between 72-82% at CCOCr, with 78% average and between 81-86% at CBO_5 with 83% average, in 2017 and 2018, is shown in Figure 7.

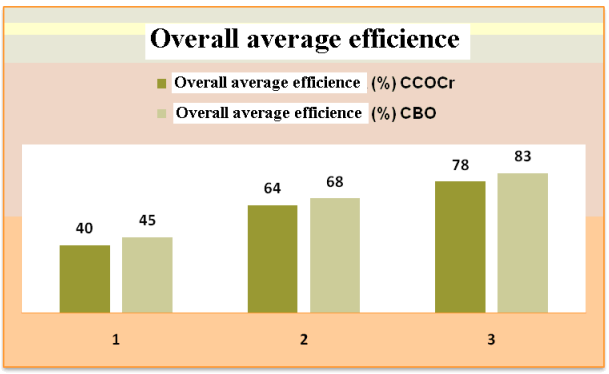

Fig. 7. *The dynamics of the average reduction efficiency of CCOCr and CBO_5 at the Galati treatment station in 2017 and 2018; 1 = mechanical step; 2 = (%) biological Step: 3 = Total installation (%)*

It is observed a superiority of the efficiency of reducing the CBO_5 to the efficiency of CCOCr reduction at both mechanical and biological treatment stages throughout the period studied, which means that the assimilated organic matter has been removed to a greater extent than unassimilated matter.

Figure 8 presents the dynamics of the Symons treatability ratio and its average value in 2017 and January-May 2018

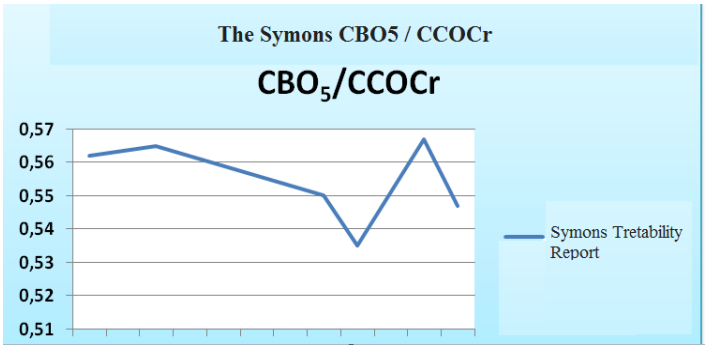

Fig. 8. *The dynamics of the Symons treatability ratio and its average value in 2017 and 2018*

The treatability ratio ranges from 0.535 to 0.567, with an average of 0.554 homogeneously depending on the loading and nature of pollutants. The reduction of Symons treatability ratio from 0.567 in the summer period to 0.535 in winter indicates that the wastewater was harder to treat during the winter period.

3. Conclusions

The reduction of CCOCr and CBO_5 from wastewater after passing through the installation of the Galati treatment station is an estimate of the quantity of organic substances removed in the treatment process.

The Symons environmental treatment ratio achieved for influence was 0.554, which framed the influence in S.E. Galati in the category of wastewater readily treatable by biological methods, in the presence of naturally occurring microorganisms in these waters. So, from the point of view of the Symons criterion, water is slightly biodegradable.

The average of the overall reduction efficiency of CCOCr is 81% and at CBO_5 is 84%, which means that also from this point of view, wastewater purified can be considered as biological treatable waters. The overall efficiency of CBO_5 reduction is a percentage value of the removal of equivalent organic matter and represents the slightly biodegradable component of global organic matter.

The efficiency of reduction of CCOCr (81%) and CBO_5 (84%) allow wastewater characterisation as biological treatable in S.E. Galati and alongside the operation at optimum parameters of treatment plants in 2017 and 2018, determines the achievement of technological performances Imposed by the legislation in force.

References

[1]. M. Negulescu, s.a., *Protectia mediului inconjurator (manual general)*, Ed. Tehnica, Bucuresti 1995.
[2]. Gabrian C. F., *Ghid de mediu*, Ed. Monitorul Oficial, 2008.
[3]. Vişan S., Angelescu A., Alpopi C., *Mediul înconjurător. Poluare şi protecţie*, Bucureşti, Editura Economică, 2000.
[4]. ***, *Poluarea atmosferică*, www.eea.europa.eu, accesat la data de 20.02.2017.
[5]. Cîrţînă Daniela, *Poluarea apelor*. Ed. SITECH, Craiova, 2005.
[6]. Gligor Delia Maria, Roşu Cristina, *Elemente fundamentale de chimia mediului*, Ed. Galaxia Gutenberg, Cluj-Napoca, 2012.

THE ANNALS OF "DUNAREA DE JOS" UNIVERSITY OF GALATI.
FASCICLE IX, METALLURGY AND MATERIALS SCIENCE
N°. 2 - 2018, ISSN 1453-083X

ANALYSIS OF THE PROPAGATION OF DEFECTS GENERATED BY THE OSCILLATION MARKS ON LAMINATED PRODUCTS

Stela CONSTANTINESCU
"Dunarea de Jos" University of Galati, Faculty of Engineering, Romania
e-mail: constantinescu_stela@ yahoo.com

ABSTRACT

In this work was followed the determination of a method of diminishing the depth of the oscillating brands and identifying how the oscillating brands can influence the surface quality of hot rolled products (backgammon and strips). This study addresses the phenomena that take place at the initiation of the crust in the crystallizer and treats the theoretical aspects of the formation of the oscillating brands on the surface of the cast products continuously. Experiments carried out have enabled to reveal aspects regarding the relationship of oscillation brands – the quality of the products (molded or laminated) and the purity of the continuous cast slabs.

KEYWORDS: segregation in Sulphur, macroscopic inclusions, fragile silicates, purity of steel

1. Introduction

The present study addresses the phenomena occurring at the initiation of the crust in the crystallization and deals extensively with the aspects of the formation of the oscillating marks on the surface of the continuously cast products [1-2]. Experiments conducted at Mittal S.A., Continuous Casting Section 1 (TC1) allowed some aspects of the oscillation brands to be revealed - the quality of the products (cast or rolled) and the purity of the continuous castings. Continuous casting is a very widespread process, whose efficiency is strictly dependent on process parameter control and the implemented construction solution. For this reason, different automated control and process control systems are used worldwide, resulting in metal removal of over 98% [3-5]. The development of the assortment and the low degree of automation of the continuous casting machines of TC1 existing castings led to the emergence of classes of defects specific to continuous casting, of which the highest weight (in terms of material downgrades) and hard to be removed are the marks of oscillation and central cracks, also known as voids. The main purpose was to determine a method of diminishing the depth of the oscillating marks. A second purpose was to identify how oscillatory marks can influence the surface quality of hot-rolled products (sheets and strips) [6-8].

2. Experimental condition

Three bits were continuously poured at Mittal S.A./TC1. Communication of all batches was: 7.6 mm amplitude; the crystallizer lubricant (Accutherm ST - C 39/4S) and the absence of the protective tube between the pot and the distributor. Characterization elements of the bats are shown in Table 1.

Table 1. *Characterization of burdens and their chemical composition*

No. charge	Steel brand	No. MTC	Speed casting, [m/min]		No. oscillations, [cicli/min]		Chemical composition, [%]					
			F1	F2	F1	F2	C	Mn	Si	P	S	Al
923657	Ol 37 - 2k	1	0.73	0.70	84	84	0.12	0.64	0.30	0.020	0.014	0.005
923658	Ust 12 Al	4	0.92	0.90	107	115	0.03	0.30	0.02	0.016	0.013	0.045
936884	43 A	3	0.48	0.51	53	74	0.17	0.98	0.25	0.016	0.015	0.005

Between the three boreholes, transverse samples were taken from castings, which were then examined macroscopically and microscopically.

3. Results and discussions

Following the reception of castings, the only surface defects detected were slag traps on the surface only at bay 923657 (4 blanks on each wire). Following the reception of laminated products, superficial cracks were found and polished on a single sheet of sheet from batch 936884. Using the calculation formulas, the negative stripping times in Table 2 were determined. Also, in this table the depth of the corresponding oscillation mark is calculated according to the relationship:

$$h = 0.0682\ e^{0.167\,\delta},\ [mm] \quad (1)$$

as well as the depth measured on samples taken.

Figure 1 shows the correlation between the formula used for calculating the oscillation marks and the depth determined by microscope measurements.

Table 2. *Negative stripping times and the depth of the oscillation mark*

No. charge	Negative stripping time, [s]		Calculated depth of the oscillating mark, [mm]		Measured depth of the oscillating mark, [mm]	
	F1	F2	F1	F2	F1	F2
923657	0.265	0.269	0.292	0.275	0.300	-
923658	0.209	0.200	0.288	0.253	-	0.225
936884	0.413	0.323	0.311	0.216	0.430	-

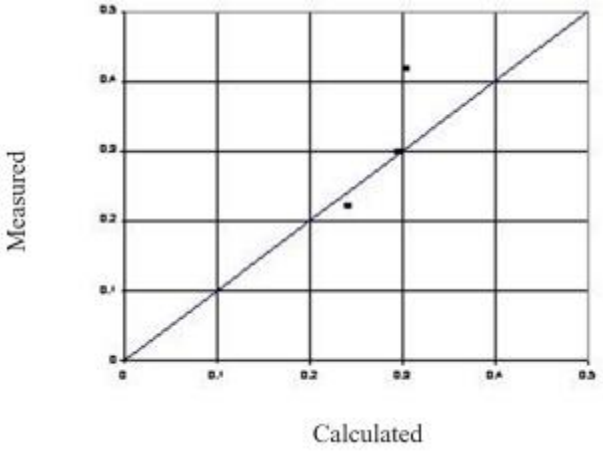

Fig. 1. *Comparison of calculated values with measured values for the depth of the oscillation marks*

The microscopic investigation of the samples taken was carried out for the highlight of the following aspects: the purity of inclusions situated at a distance of approx. 20 mm of slab surface, considering this quota as the maximum possible limit of crystallization influence (thickness of the crust at the output of the crystallization, for charges followed between 8-12 mm); the purity of the inclusions in the area of the oscillating brands (the area with a depth of approx. 5 mm from the surface; the solidification structure in the oscillating brands area.

3.1. Purity of inclusion in the area approx. 20 mm from surface sleb

The samples taken were analysed in cross section, on a direction perpendicular to the upper face of the slab. The analysis was accomplished by completing the entire thickness of the sample and counting the number of microscopic and macroscopic inclusions on each microscopic field.

It was observed that the maximum number of inclusions is placed in the field 10-15 mm from the slab surface. Macroscopic inclusions located in other areas than oscillating marks were observed only in the sample of charge 923657, i.e. 15 mm from the surface: 2 INM ø 40-80 µm and 1 INM ø > 80 µm. In this analysis it was started from the fact that the inclusions under 40 µm are endogenous, and those over 80 µm are exogenous. The investigation of the sample of charge 936884 in two parallel planes with the superior face of the slab, located at the rate of 5 and 15 mm, with dimensions 25 x 45 mm,

emphasized that the problem of concentration of inclusion is not a local accident.

3.2. Purity of inclusion in the area of the oscillating brands

The purity analysis of all the samples in the area of the oscillating brands has emphasized, at charge 936884, the existence of the inclusion strings embedded in "hook" formed during negative stripping, in Figure 2 It is observed that the length of these strings does not exceed 100 μm. This phenomenon is characteristic of the entire sample analysed.

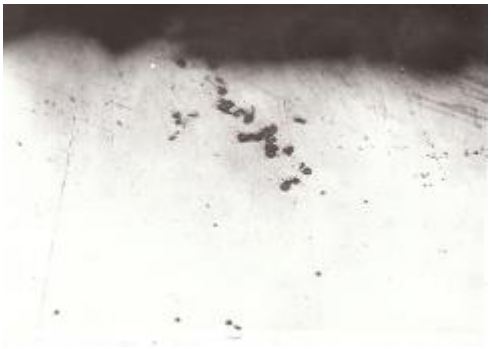

Fig. 2. *Non-metallic inclusions on the oscillation mark – charge 936884 – X250*

Fig. 3. *Group of non-metallic inclusions in the right of oscillation mark – charge 936884 – X 50*

Also, at this charge it was observed in the area of the oscillating brands, a group of macroscopic inclusions positioned at 3-4 mm from the surface. The appearance and layout of this grouping is shown in Figure 3.

The microprobe analysis of these grouped inclusions has emphasized the following: the inclusions have an aluminum base component; the following components as weight are magnesium and calcium; silicon content does not differ from the value of the base material (the content of Si inclusion is close to that of the steel). The results of the analysis are presented in Figures 4-9.

Fig. 4. *Composition image, X300*

Fig. 5. *Image of secondary electrons, X300*

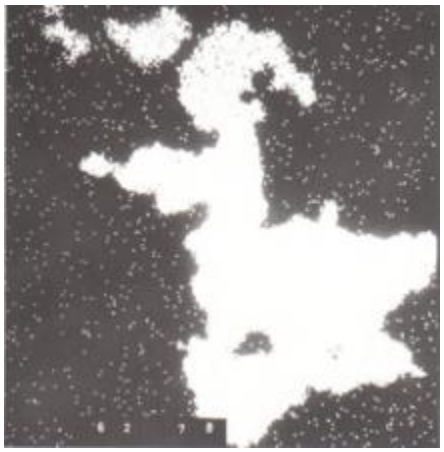

Fig. 6. *Distribution Al, X300*

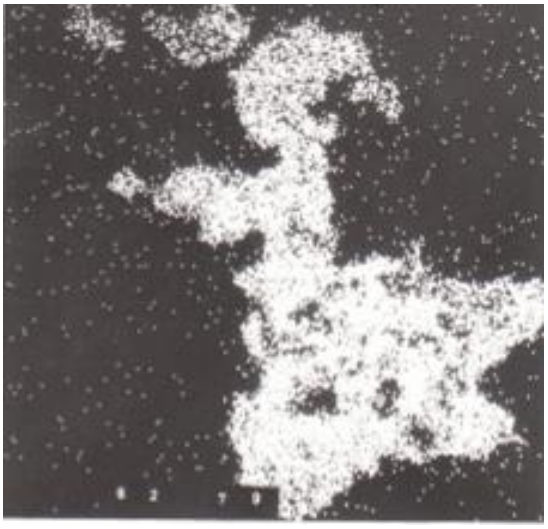

Fig. 7. *Ca Distribution, X300*

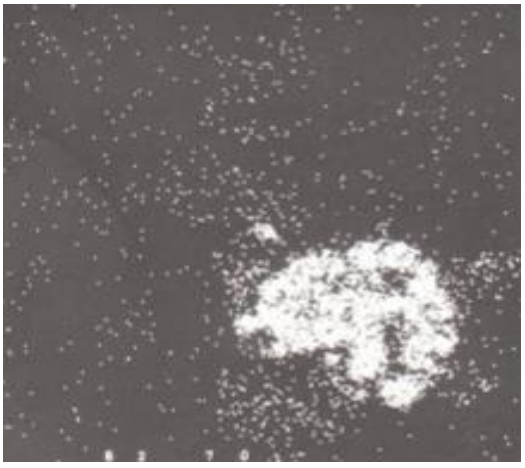

Fig. 8. *Mg Distribution, X300*

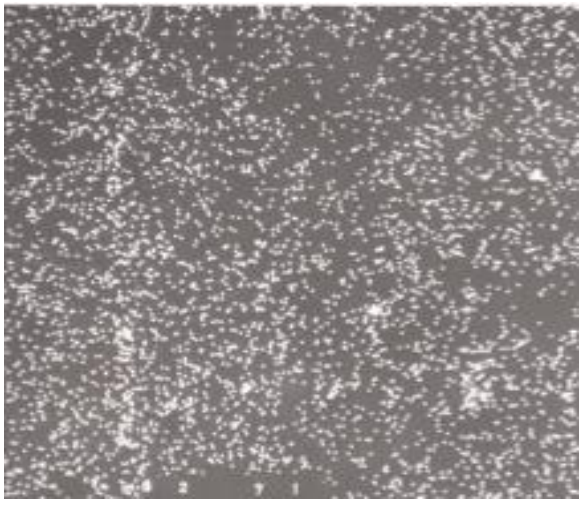

Fig. 9. *Si Distribution, X300*

3.3. The appearance of the hardening structure in the oscillating brands area

The analysis of the hardening structure in the area of the oscillating brands emphasized the following: at charge 936884 it was observed the presence of "hooks", Figure 10. At charge 923658 these "hooks" were virtually non-existent - Figure 11; Macroscopic inclusions analysed for charge 936884 9 (Fig. 3-9) were not retained by the deformation of the crust during the negative stripping, Figure 12.

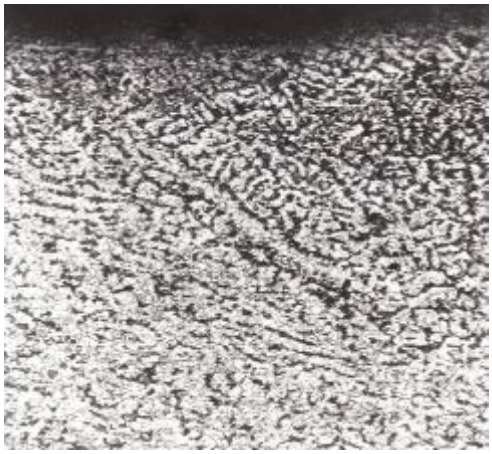

Fig. 10. *Hardening structure in the right of the oscillating mark at charge 936884 – X 100*

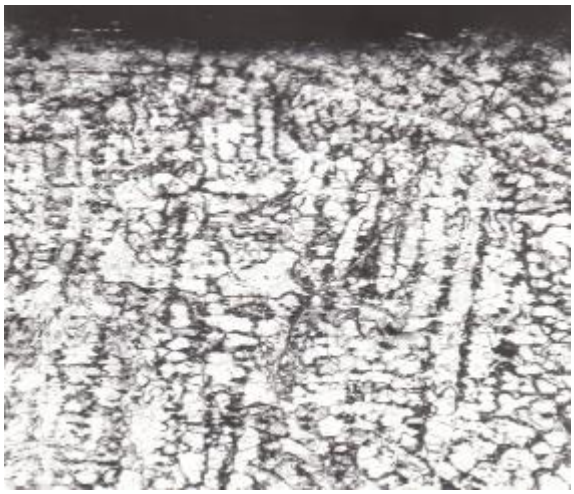

Fig. 11. *Hardening structure in the right of the oscillating mark at charge 923658 – X 100*

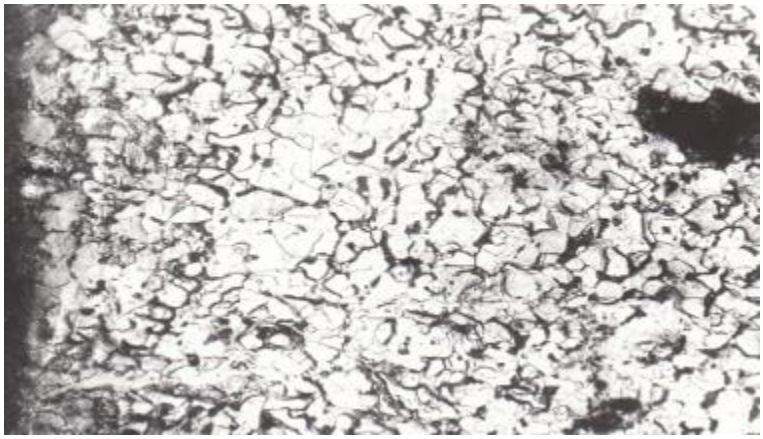

Fig. 12. *Solidifying structure in the area of macroscopic inclusions - charge 936884 – X100*

4. Conclusions

Oscillating marks cannot be considered as deceiving a defect, they are characteristic of continuous casting.

Oscillating marks may be an additional cause in the appearance of cross-sectional cracks, in conditions where the formation of the crust has been defective (deep oscillating brands with strong crust deformation and inclusion in the area of scarring).

Inclusions, especially exogenous ones, can be caught, now of negative stripping, in a subcutaneous area with a thickness of approx. 100 µm, as is apparent from the Figures 2 and 10.

Concentration of endogenous inclusions in an area of max. 20 mm thickness from the surface of the sleb is the characteristic to the curved wire casting machines. The only possibility to correct this is to ensure the purity of the upstream steel. These inclusions will affect the quality of the laminate product surface.

References

[1]. Stanciu C., *Research on the performance of system for measuring the cooling speed of brams and blums continuously cast*, S.C. ICPPAM Galati, 1995.
[2]. Stanciu C., *Researches for the implementation of temperature-discontinuous measurement systems in the casting pot*, S.C. ICPPAM Galati, 1994.
[3]. Constantinescu S., *Researches on the effect of the tempering on both structure and properties of thick plates*, Metalurgia International, vol. IX, no. 6, p. 12-16, 2004.
[4]. Walanbe T., *Mechanical properties of Cr-Mo steels after elevated temperature service*, 1st part.: Document II S-IX-116-79, 2nd part.: Document II S-IX-1167-1990.
[5]. Sugiyama T., *Kobe steel engineering raport*, vol. 25, no. 4, 1995.
[6]. Constantinescu S., *Influence of manufacturing process on chemical and structural homogeneity of welded pipe sheets for tanks and vessels working under pressure*, Processing Technologies, September 18-21, 2001, Leganes, Madrid, Spain.
[7]. Taffner K., *et al.*, Symposium low alloy high strength steel, Nuremberg 21-23 May 1990.
[8]. Morrison W. B., *et al.*, *Controlled process of high strengh low alloy steels*, New York, 1996.

THE ANNALS OF "DUNAREA DE JOS" UNIVERSITY OF GALATI.
FASCICLE IX, METALLURGY AND MATERIALS SCIENCE
N°. 2 - 2018, ISSN 1453-083X

FUSIBLE MODELS USED TO CASTING SMALL DIMENSIONS SCULPTURES

Bogdan MURARIU[1]*, Beatrice TUDOR[2]
[1] "Gheorghe Asachi" Technical University, Iasi, Romania
[2] "Dunarea de Jos" University of Galati, Faculty of Engineering, Romania
*e-mail: bogmurariu@gmail.com

ABSTRACT

During the study regarding the obtaining of artworks using light fusible models it has been highlighted the possibility of dividing the process of casting-molding in simple, separate operations, whose execution becomes accessible even to people with no high qualification in the field.

An important realization during the study is represented using the dental molding- packaging mass, which has ensured the obtaining of the smoothness of the surfaces and the clarity of form's configurations.

Designing the casting network has been the main preoccupation, in order to ensure the complete action of emptying the wax from the mould and filling it correctly with metal.

A special attention has been granted to cleaning and finishing the surface of the sculpture, this operation ensuring the texture of the future artwork.

KEYWORDS: model, packaging mass, bronze, mould, casting network, cleaning, finishing

1. Introduction

Obtaining cast pieces using fusible models has its origins in the activity of those working in the field of art and today, among other casting technologies, it is a widely used technique in the foundries.

Due to its age of practice, it is difficult to give a precise period of discovery of the casting with fusible models and it is impossible to know the origin and the way of its birth.

Sources point at Egypt and China as countries where this technique has been invented around 3000 B.C. Initially the method was used to cast metals having low melting temperatures (gold, silver, bronze) and in casting jewelleries or artworks.

Having on its side the manufacturing aspect, the technique has special advantages to offer for the nowadays sculptor.

Fusible models can offer the possibility of casting pieces with intricate forms, reduced thickness of the walls and a special look of the surfaces, offering in the same time a great freedom in realizing of forms inviting the artists to unleash his imagination.

The advantages of this method are unquestionable: perfect copying of the tiniest details, obtaining trenches directly from casting, outstanding state of surfaces, mechanical or chemical easy finishing of the cast pieces, aligning with the environmental protection regulations. Adding to these the disappearance of other technologies' imposed constraints as the possibility of obtaining artworks with complex forms or the possibility to obtain the finest details, absolutely necessary for an artwork, or using less quantities of material during the process of moulding-casting the utility of this casting technique regarding sculptures is obvious.

Besides, the technique is as simple as it could be, but a little costly. The casting worker is as important as the sculptor and could contribute to the fame of the sculptor [2, 4].

2. Studies Regarding the Casting of Sculpture Works with Fusible Models

It is well known the fact that casting one piece requires a model, its realization being done by the modeler who builds it following the instructions from a drawing. Concerning the artwork, the sculptor is the one who builds from wax a model which must be the same as the final sculpture, his activity being the warranty of a quality original artwork (Fig. 1 and Fig. 2).

Fig. 1. *"Samurai"*

Fig. 2. *"Knight IV"*

For the study undertaken, I have realized two models, replicas of the desired sculptures, which would be the basis of two statues with the help of fusible models realized in wax (Fig. 3 and Fig. 4).

Fig. 3. *Wax Model for the Casting of the "Samurai"*

Fig. 4. *Wax Model for Casting of "Knight IV"*

The reason for choosing the casting method using moulds with fusible models was not to obtain geometrical precision (low tolerances) but obtaining a clear copy of the artwork' configuration.

The fusible models had to correspond to all requirements of this technique (building the mould, evacuation of the wax, and pouring of the alloy, etc.), the quality of the cast piece depending on accomplishing these requirements [1, 3].

Realizing the channels of the casting network to fill the mould with molten metal and the gases evacuation from its interior is a very important operation because its good functionality is the key to successfully fill the cavities with bronze as well as evacuating the gases from its interior. The elements of casting network were modeled also from wax, being added afterwards to the fusible model. A special attention needs is required when doing this operation, any mistakes being able to lead to overheating and deformation of the model.

The cross section of the feed channels is usually circular, their diameter being particularly important and having to be in correlation with the size of the piece to be cast [5].

In the industrial practice, in series casting, there are calculations done to obtain the right dimensions of these, according to dimensions, walls' thickness and type of alloy. In the case of artworks, another way of doing the calculation is made, based on experience, intuition and a correct approximation of its dimensions. For artworks with dimensions similar with my models', sculptors considering this calculation system appreciate the diameter of the cross section being approximative 0.8 cm.

Fig. 5. *Casting network for the casting of the "Samurai"*

Fig. 6. *Casting network for the casting of the "Knight IV"*

Feeding channels have been realized with variable cross sections, decreasing towards the contact zone with the main piece in order to assure normal filling speed. At the contact point with the mould cavity, the cross section of the feeding channels is not supposed to be much larger than the thickness of wax wall, casting defects being favoured to appear in the cast piece otherwise due to contractions differences [7].

Many principal feeding channels have been utilized connected to the casting funnel, considered enough compared to the sizes of the cast artworks, these channels having ramifications connecting with the wax model at different levels.

Another important component of this casting network necessary to casting is the channel is the ventilation duct. This one, or these ones, supposing that there is one or many, vital for successful casting, have the role of evacuating the gases accumulated in the mold's interior when the molten metal is in contact with the mould. They have been built also from wax, having reduced diameters, serving only for evacuating the gases.

Plaster moulds have been chosen to cast the pieces because of the advantages over the classic ones, and because of the fact there was no casting mixture to be mechanically pressed which could lead to deteriorated models, plaster getting hard by itself, chemically. Other advantages are linked to obtaining cast pieces with very smooth surfaces, they are cheaper compared to other precision methods, and finally they offer the possibility of casting pieces with thin walls [6, 8].

The plaster as moulding material commonly used in foundries has a series of features which make the moulds to have some advantages. The pieces have a rough structure, so they have mechanical features which are reduced, and, in the case of an artwork, they do not matter because of reduced thermal conductivity and low permeability, so leading to a raised possibility of appearance of sulphides.

During the study I have used investment material used in dental technology which assures supplementary advantages compared to the industrial one: high fluidity, good resistance, minimal changes in volume due to temperature variations.

In the case of industrial gypsum, the moulds need to dry in the air for 24 hours in order to solidify. The other operations linked to obtaining the mould like melting and evacuation of the wax, getting the moulds dry and the calcination require a period of 30 hours.

On the contrary, the dental investment mass gets to fully solid mould and at a resistance level in humid state high enough in order to be put in the oven in a period of only few hours. Even if the wax melting temperature is around 63-70 ^{o}C, its complete removal from the moulds requires higher values of the temperatures. If the evacuation is not complete, the small particles of the residues retained on the finest zones of the moulds are an obstacle in obtaining a real artwork. The longer the time in the oven, the better the evacuation of the residues from the mould cavity.

It is desirable for the wax evacuation to be done in 2 stages. The wax evacuation would be done having the casting funnel facing downwards, and when the wax has been evacuated almost entirely, the mould should be positioned with casting funnel facing upwards in such a way that the oxygen (from

the oven) should circulate more easily reacting with the wax and realizing gases, which are evacuated, and not Carbon particles.

Time to be exposed in the oven should be longer if the temperature in the mould is lower and the size of wax larger. In the case of dental investment material, it could be introduced in the pre- heated oven even if the temperature is 500 °C without the danger of cracks appearance.

In the Figures 7 and 8 are presented the moulds used for casting the two statues.

***Fig. 7, 8**. The moulds used for casting the two statues*

The alloy casting has been done gravitationally, this method being the most used one in the foundries. The estimated quantity of metal necessary for the casting has been done considering the model's volume having as data calculation the weight and density of the wax being used.

The alloy has been melted in an oven with induction, its temperature being 1200 °C. After the casting and cooling, the hammering followed. The casting funnel and network have been removed the first, the pieces being afterwards finished through sanding.

In order to ensure that the surfaces and the parts with large bumps (Figures 7 and 8) are perfectly smooth and to ensure the model's configuration after cleaning, I realized a finishing with the chisel, the rasp and abrasive discs.

Final touch has been realized in several stages, starting with a preliminary processing with a new rasp, followed by successive sanding stages done with different sandpapers of different granulations in descending order (large, medium and fine respectively).

This finishing has been of extreme importance, the final aspect of the artwork depending on it, requiring a large amount of working and patience. As a casting worker and a sculptor, the surface smoothness must be compared with the metallographic samples.

3. Conclusions

The mould mixture used to build the mould has been a dental investment material, a little expensive which ensured a high quality level of the cast piece as well as a shorter period of time on the entire cycle of utilizing it, starting with building the mould and ending with removing the artwork from the mould.

Realizing the moulds from plaster, which hardens chemically, creates the conditions to avoid the action of tapping the sand mixture and deteriorations of the model or leading to vibrations during moulding.

Slower solidifying of the alloy as a result of low thermal conductivity of plaster moulds and the ore pronounced tendency of the artworks to form voids and rough structure have been prevented by a casting network where the stress was on the feeding channels.

References

[1]. Radulescu C. Gh., Albita Gh., *Retele de turnare*, Editura Tehnica, Bucuresti, 1976.
[2]. Florea Gh., *Procedee performante de punere in forma*, Editura Europlus, Galati, 2008.
[3]. Buzila S., *Procedee speciale de formare*, Editura didactica si pedagogica , Bucuresti, 1978.
[4]. Florea Gh., Chiriac Al., Marginean I., Croitoru Gh., *Turnatoria de Arta Foundry*, Materiale metalice, Partea I si II: Editura Europlus, Galati, 2008.
[5]. Robert G. Craig, *Materiale dentare restaurative*, Editura All, Bucuresti, 2001.
[6]. Simionescu Gh., *et al.*, *Ingineria proceselor de formare*, Editura Alvarom, Bucuresti, 2000.
[7]. Carcea I., Matei Gh., *Aliaje neferoase de turnatorie*, Editura Performantica, Iasi, 2000.
[8]. Elisabeta Vasilescu, Ana Doniga, *Modern Approaches in Design Optimization of Parts and the Development Trend of Surface Treatments*, Analele Universitatii Dunarea de Jos din Galati, Fascicula IX Metalurgie si Stiinta Materialelor, nr. 9, p. 30-36, 2012.

THE ANNALS OF "DUNAREA DE JOS" UNIVERSITY OF GALATI.
FASCICLE IX, METALLURGY AND MATERIALS SCIENCE
N°. 2 - 2018, ISSN 1453-083X

MODIFYING THE STRUCTURE AND SURFACE PROPERTIES OF Ti6Al4V ALLOY BY CARBONITRIDING IN FLUIDIZED BED

Nelu CAZACU
"Dunarea de Jos" University of Galati, Faculty of Engineering, Romania
e-mail: nelu.cazacu@ugal.ro

ABSTRACT

The Ti6Al4V alloy is known as being one of the most widely used biocompatible alloys and not only that. The study is based on experienced research of the hardening in a fluidized bed and applied to samples of Ti6A14 in laboratory conditions. The carbonitriding has been accomplished on an exterior electric heating reactor. It has been examined the influence of the heat and the duration of the thermochemical treatment out of economy interests, the flow has been made with a mix of CH_4 and NH_3 (5% concentration). The results have been examined through hardness (HV5), metallographic microstructures and micro hardness in section (micro HV).

KEYWORDS: titan alloy, Ti6Al4V, carbonitriding, FBT, Fluidized bed

1. Introduction

Carbonitriding represents a thermochemical treatment, with a wide application on steels because of the advantages it has concerning the modifications of chemical structure and superficial properties, after the application of a hardening and return treatment. A primary treatment applied to the surface is recommended on steels to put the value of the resources after the carbonitriding.

The influence of different types of superficial (1) has been studied, such would be the lustre, the sanding, the processing with steel shots of samples of Ti6Al4V before the carbonitriding made in plasma.

The insertion of argon gas and spraying with carbon atoms from a graphite damper in the plasma workspace [N_2-Ar-C (g)] can lead to the production of the desired nitrate, phases of carbide and nitrocarbide on the surface and inside titanium alloy samples and can lead to changes in the microstructure. That is why the samples have been carbonitrided in N_2/Ar (70% N_2 + 30% Ar) plasma at a 650 °C temperature, for 5 hours. The carbon atoms have been generated in the graphite hollow cathode, where carbon atoms spraying takes place, during the nitriding process. The results lay out the facts that there exists a forming of a thicker layer of TiN and

The hardness after carbonitrating in fluid layer depends on the duration of the treatment and the working temperature. Carbonitrures in the sample are blown with sand but with irregular topography. The samples processed with steel shots and the polished ones have smoother surfaces, while the nitride and carbonitride layer is smaller. The hardness of the Ti6Al4V carbonitrided alloy on a 650 °C temperature could get to values close to 850 HV on the surface and gradually decreases till the substrate value (300 HV).

Another example is nitriding and nitrocarburizing of gun pipes (2). A gun pipe made of titan alloy (Ti6Al4V) has been nitrocarburized in a fluidized bed at a rough 788 °C temperature for 6 hours. The composition of the reacting gas was: ammonia (NH_4) 50%, natural gas (CH_4) 5% and nitrogen 45%. The result has been the obtaining of a pipe with a nitrocarburized surface. Its characteristics were the following:

- increase in the projectile speed;
- the pipe had a smooth finish;
- the pipe had a reduced friction;
- the pipe had a bigger wear resistance;
- the hardness of the pipe was significantly increased;
- the distortion resistance of the pipe was a good one even after repeated shots;
- the corrosion resistance was improved.

Notations and abbreviations
FB – Fluidized Bed
FBT – Fluidized Bed Technology
CN – CarboNitriding
FBCN – Fluidized Bed CarboNitriding

One of the advantages of using the fluidized oven and funnels at the edges of the titanium pipe is that the processing time for completion of the same results in a fluidized oven is reduced from 24 hour to 6 hours, and the temperature is reduced from 980-1010 °C to 760-870 °C. This decrease of temperature is considerable for the treatment of a titan alloy pipe or any titan alloy because it is a lot under the melting point. And so, the distortion risk has been importantly reduced or even deleted.

The Ti6Al4V alloy treatment by ionic carbonitriding was studied regarding the moulder of nitrides and carbides layer through. To this purpose, there has been used a plasma room of nitriding and a hollow graphite cathode using nitrogen and argon. The titanium samples and Ti6Al4V have been carbonitrided in plasma N_2-C (g), at temperatures between 500 °C and 1000 °C. The generation of gas carbon in the plasma atmosphere is possible through ionic bombardment of a graphite target strategically emplaced in the interior of the room. The results indicate the fact that the N_2-C atmosphere is suitable to such a treatment type, creating layers of TiN, T_2N and $TiC_{0,3}N_{0,7}$, compounds with the thickness of about 2.0 μm when the treatment is made at low temperatures (550-600 °C) and 35.0 μm for treatments at higher temperatures (1000 °C).

The achievement of carbonitriding of Ti in fluid state respects Fig. 1 such as using initial precursors, marsh gas and ammonia stable in normal conditions. At the conditions of the thermochemical, the instable thermodynamic precursors decompose (Fig 1).

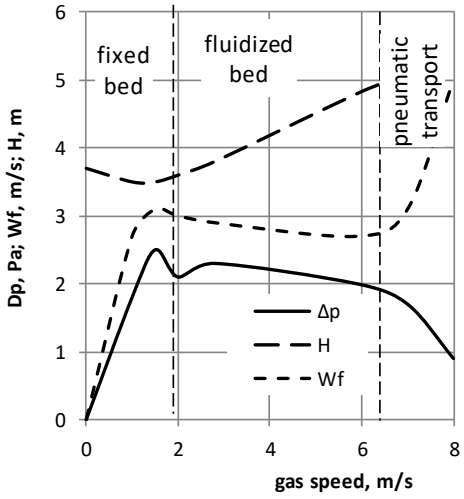

Fig. 1. *The fluidized bed is limited by the fixed bed and the pneumatic transport*

The employment of the flow layer at thermochemical treatments applied in superficial modifications is made with the following remarks:

- the environment of the flow layer is thermally active and chemic in some gas dynamic functioning conditions
- the environment of the flow layer is characterized by a high consumption of technological gases, because the resulted gases and the initial coloured traces also provide the flow phenomenon.
- the impact of the carbonitriting in flow layer technology over the environment is practically reduced at a small quantity of CO_2+steam of water that results after the final combustion of the fuel substances at the reactor exit.

2. Experimental conditions

The objective of the experiments in laboratory condition has been made to emphasize the possibility of superficial modifications concerning the Ti6Al4V alloy. Furthermore, it tracks the capacity of the medium to create a thermal activity and a chemical one by controlling some technological factors.

Experimental model is realized so that physics and specific chemical phenomena can be highlighted: fluidity, the thermal and chemical decomposition of the chemical reactions (Fig. 1, Fig. 2).

There have been used samples of Ti6Al4V alloy taken from a material used to making dentures. The material is made by the Zeno corporation (Germany) having the chemical composition and the properties guaranteed in the following table:

chemical composition of the Ti6Al4V alloy is being presented in the (Table 2).

Table 1. *TI6Al4V alloy characterization*

Type Titanium Alloy grade 5	u.m.	
Density	g/cm3	4.3;
Vickers Durity	HV 5/30	350;
CTE (25 - 500 °C)	10-6 K-1	10.3;
Constituents	%	Al : 5.5 - 6.75
		V : 3.5 - 4.5
		More : <0.4
		Rest : Ti
Limit Break	Mpa	930
Tehn Limit of Elasticity 0,02	MPa	900
Elongation		10
Melting point	°C	1604 - 1660
	F	2919 - 3020

The samples have been cut and finished on vertical surfaces with sandpaper 300. The vertical surfaces are the ones that are important for the thermochemical treatment in fluid layer. The samples have been tied with wire to a loading device. It is known the position influence of the surfaces of the oven, which is important at thermal treatments and thermochemical treatments in fluid layer and not

only. The following step consists of emplacing the samples of Ti6Al4V alloy in the middle of the fluid layer. In the carbonitriding in fluidized beds process it is necessary that the following factors be taken into consideration:

- samples positioning in the oven
- carbonitriding temperature.
- the duration of the process.
- the chemical activity of the environment (concentration of ammonia or flow of ammonia).

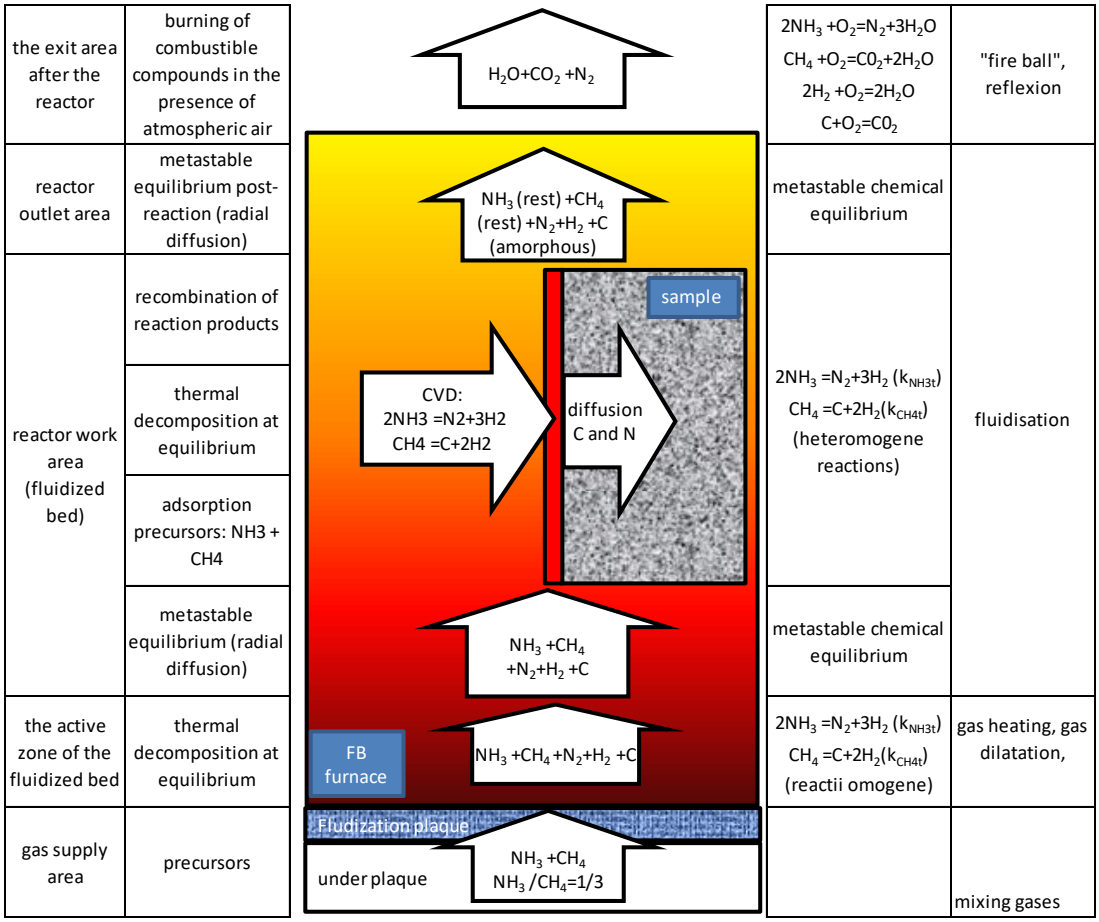

Fig. 2. *Physical and chemical processes on fluidized bed nitrocarburizing*

For the development of the experiments it has been used a classical factorial matrix, taking into consideration the following factors and the following levels: temperature: 930 °C; 850 °C; 750 °C and treatment duration: 60 min; 90 min; 120 min (Table 2). The relatively small durations of treatment are due to the chemical and thermal activities of the environment which are higher than when done in gas and smaller than the ones in salts baths, and the fact that the loading and unloading are done much faster due to working with an open enclosure.

Table 2. *Experimental regimes for FBNC applied to Ti6Al4V alloy samples*

exp. no.	temperature	time	gas composition
u.m.	°C	min	%
1	750	60	95% methane + 5% amoniac
2		90	
3		120	
4	850	60	
5		90	
6		120	
7	930	60	
8		90	
9		120	

3. Results and dissection

The structural changes have been analysed through metallographic analyses. The samples are sectioned at about ½ from their original height (original height of the disc). Investigation methods follow:

- pointing the chemical modifications on the surface and the chemical composition profile from the surface to the core;
- pointing the structure modifications on the surface and the transition zone towards the core;
- pointing the properties modifications on the surface and the transition zone to the core.

The investigations have been conducted in laboratory on significant samples, in standard stated conditions and have been conducted through:

- microstructure in transversal section for highlighting the structural modifications which determine the superficial properties modifications;
- Vickers hardness on surface, for highlighting superficial properties modifications.

The Ti6Al4V alloy samples have been sectioned at half their height and have been emplaced in two-component resin. After hardening, the grinding was achieved manually using sandpapers. The polish took place on moist felt with the polish agent 3-A-S.

The metallographic attack has the role of highlighting the structure elements in the new section. That reacts with the surface of the sample differentiated depending on the microrelief and the local free energy. The image obtained with the help of the metallographic microscope in different sizes highlights structural constituents, flows and superficial thermo-chemical treated zone.

The most used chemical reactive for the metallographic attack of titan and titan alloys is the Kroll reactive which has the following chemical composition: 100 ml distilled water, 1-3 ml hydrofluoric acid, 2-6 ml nitric acid.

The reagent concentration may vary in wide scales depending on the alloy type. The reagent gives a dark brown coloration for the β phase.

Titan can be attacked and coloured using the Weck reagent, which has the following chemical composition: 100 ml distilled, 5 g ammonium biflorure.

The microstructure in the transversal section was made on the un-attacked surface for highlighting inclusions and on the attacked surface

In Fig. 5 to 13 are presented the representative microstructures for the nine probes carbonitrated in fluidized bed.

Fig. 4. *Sample Ti6Al4V attacked with cu Kroll reagent*

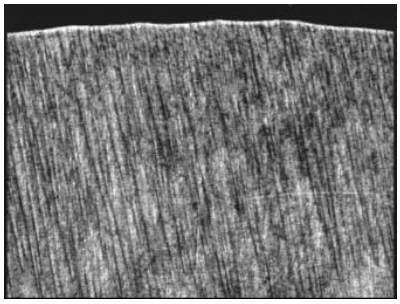

Fig. 5. *Microstructure of the first sample of Ti6Al4V alloy corbonitrided at 750 °C/60 min (zoom: 100x)*

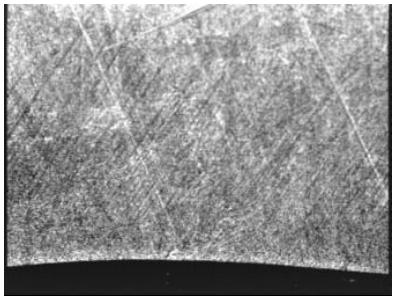

Fig. 6. *Microstructure of the second sample of Ti6Al4V alloy corbonitrided at 750 °C/90 min (zoom: 100x)*

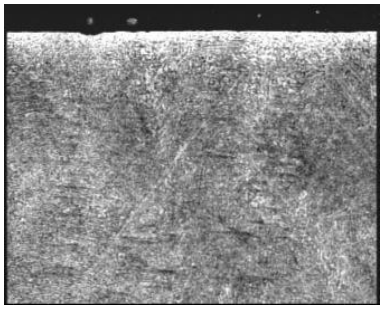

Fig. 7. *Microstructure of the third sample of Ti6Al4V alloy corbonitrided at 750 °C/120 min (zoom: 100x)*

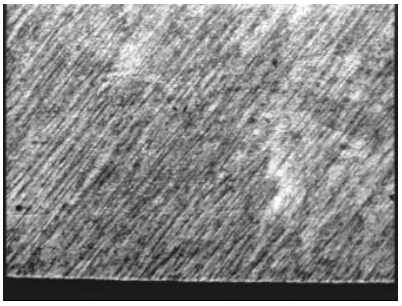

Fig. 8. *Microstructure of the fourth sample of Ti6Al4V alloy corbonitrided at 850 °C/60 min (zoom: 100x)*

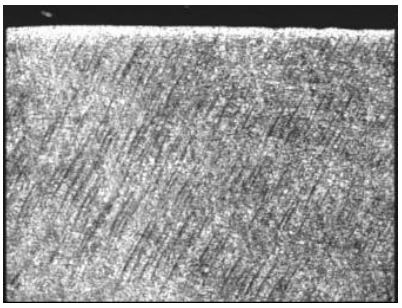

Fig. 9. *Microstructure of the fifth sample of Ti6Al4V alloy corbonitrided at 850 °C/90 min (zoom: 100x)*

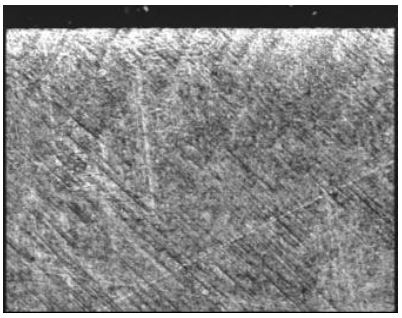

Fig. 10. *Microstructure of the sixth sample of Ti6Al4V alloy corbonitrided at 850 °C/120 min (zoom: 100x)*

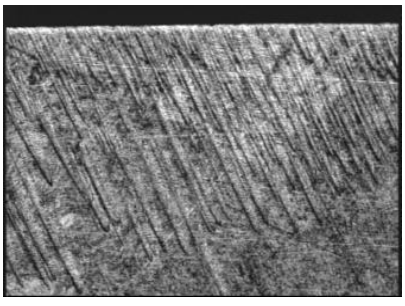

Fig. 11. *Microstructure of the seventh sample of Ti6Al4V alloy corbonitrided at 930 °C/60 min (zoom: 100x)*

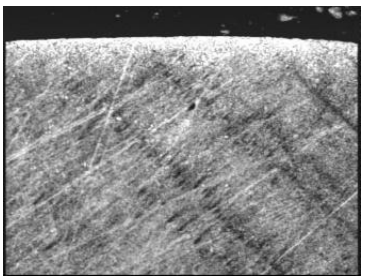

Fig. 12. *Microstructure of the eight sample of Ti6Al4V alloy corbonitrided at 930 °C/90 min (zoom: 100x)*

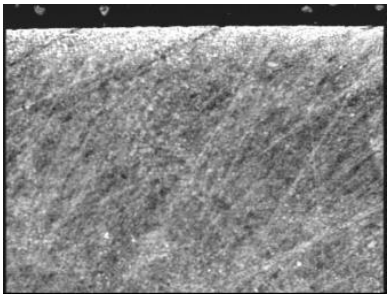

Fig. 13. *Microstructure of the ninth sample of Ti6Al4V alloy corbonitrided at 930 °C/120 min (zoom: 100x)*

Table 3. *Medium layer depth for Ti6Al4V carbonitrided in fluidized bed (FBCB)*

sample	time	temperature	depth layer
m.u.	min.	°C	mm.
1	60		0,01
2	90	930	0,02
3	120		0,03
4	60		0,01
5	90	850	0,03
6	120		0,03
7	60		0,01
8	90	750	0,02
9	120		0,02

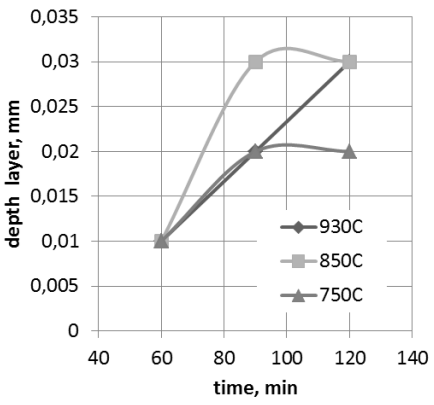

Fig. 14. *Ti6Al4V Layer depth after FBCN*

Table 4. *HV5 Vickers hardness after CNFB*

Sample Nr	d^2	HV_5	HV Final	Temperature	Time
u.m.	mm	daN/m^2	daN/m^2	°C	min.
1	0.142	459.83	437.48	930	60
	0.149	417.64			
	0.146	434.98			
2	0.146	434.98	435.02	930	90
	0.147	429.08			
	0.145	441.00			
3	0.145	441.00	515.03	930	120
	0.151	406.65			
	0.115	697.45			
4	0.139	479.89	466.70	850	60
	0.144	447.15			
	0.140	473.06			
5	0.129	557.18	535.41	850	90
	0.135	508.75			
	0.131	540.29			
6	0.121	633.29	695.64	850	120
	0.111	752.54			
	0.115	701.10			
7	0.147	429.08	425.58	750	60
	0.145	441.00			
	0.151	406.65			
8	0.130	548.64	566.19	750	90
	0.128	565.92			
	0.126	584.03			
9	0.142	459.83	439.49	750	120
	0.149	417.64			
	0.145	441.00			

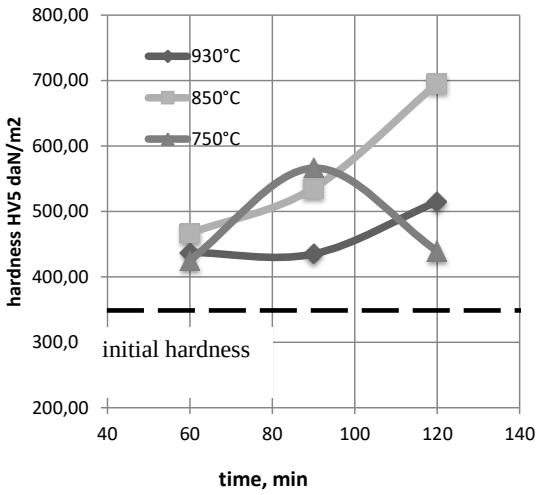

Fig. 15. *Hardness after BFNC*

The Ti6Al4V alloy hardness after carbonitrating in fluidized bed are shown in table below and interpreted in Fig. 13.

The hardness after carbonitrating in fluid layer depends on the duration of the treatment and the working temperature.

3. Conclusions

- A carbonitrating layer develops on all Ti6Al4V alloys after all experiments of carbonitrating in fluid layer;
- the hardness of the Ti6Al4V alloy after carbonitriding in fluidized bed increases on all experimented samples;
- the hardness after FBCN increases with the carbonitriding temperature;
- for every treatment temperature the hardness has a maintenance duration of maximum 2 hours;
- there has been observed a maximum in increasing the layers thickness and its hardness at 850 °C, for a 2-hour duration (Fig. 9).

References

[1]. Comunello N. J., da Rosa T. R., Fontana L. C., São José dos Campos, Universidade do Estado de Santa Catarina, Joinville, s.n., SC – march 2007.

[2]. Kunin Stephen G., *Bibliography, U.S. Patent, Method for nitriding and nitrocarburizing riffle barrels in a fluidized bed furnace*, Stephen G. Kunin – Acting Commisioner of Patents and Trademarks- 1993, USA, 1993.

[3]. Carţiş I. Gh., *Tratamente termochimice*, Timişoara: Facla, 1988.

[4]. Cazacu N., *Cercetări privind tehnologia de tratament termic în strat fluidizat pentru semifabricate siderurgice şi piese (doctoral thesis)*, Galaţi: Universitatea „Dunărea de Jos", 2000.

[5]. Cazacu N. *et al.*, *Carburarea în strat fluidizat*, Galaţi: Editura Fundaţiei Universitare „Dunărea de Jos" Galaţi, 2001.

[6]. Aloman A., *Materialologia titanului*, Bucureşti: Editura BREN, 2001.

THE ANNALS OF "DUNAREA DE JOS" UNIVERSITY OF GALATI.
FASCICLE IX, METALLURGY AND MATERIALS SCIENCE
N°. 2 - 2018, ISSN 1453-083X

IMPROVING THE POWERFUL BEHAVIOR OF AN EXPERIMENTAL MODEL OF SAVONIUS TURBINE (S-ROTOR) WITH COUPLED AERODYNAMIC ADDITIONAL BLADES

Nelu CAZACU
"Dunarea de Jos" University of Galati, Faculty of Engineering, Romania
email: nelu.cazacu@ugal.ro

ABSTRACT

The proposed experimental model brings an improvement in the start of turbine rotation and torque uniformity in load. Constructively, the original blades of the turbine have gap and overlay. Additional blades are placed at 90° from the classic layout of the blades at the Savonius turbine and are attached to the original blades. The model was tested on the wind tunnel at low wind speeds (<4.5 m/s). The results confirm the validity of the concept, without significantly increasing the yield of the experimental model.

KEYWORDS: Savonius Turbine, S-rotor, adjacent blades

1. Introduction

The Savonius wind turbine with a level (1L) and two blades or a pair of blades (1PB) is perhaps the simplest structure. From a gas-dynamic point of view, the hemispherical blades offer the maximum torque when they have a diametrically planar plane perpendicular to the wind direction. This is because the coefficients of drag (drag) for the spherical cup in the convex position c_D = 0.3 and for the concave position c_D = 1.2. The values are taken in relation to the disc with the same surface as the cup bases.

Like the semi-cylindrical blades, which are easier to obtain, for the axial plane comprising the bases of the semi-cylindrical blades, perpendicular to the wind, the highest torque value is obtained [1].

Wind energy is pure kinetic energy and can be partially transformed into mechanical work [2, 3].

$$E = 0{,}5mv^2 \tag{1}$$

The volume flow over the swept area is:

$$\dot{V} = Av \tag{2}$$

And the mass flow is:

$$\dot{m} = \rho Av \tag{3}$$

The power of wind is depending by wind speed (v), air density (ρ) and swept area (A):

$$P = 0{,}5\rho Av^3 \tag{4}$$

For the VAWT, the Betz limit is (14.81%) [2].

The power extracted from a wind power by a VAWT Savonius type is depending by Drag force is:

$$D = C_D \frac{1}{2}\rho(v-u)^2 A \tag{5}$$

where *u* is tip speed of blade. P becomes:

$$P = Du = C_D \frac{1}{2}\rho v^3 (1-\frac{u}{v})^2 \frac{u}{v} A \tag{6}$$

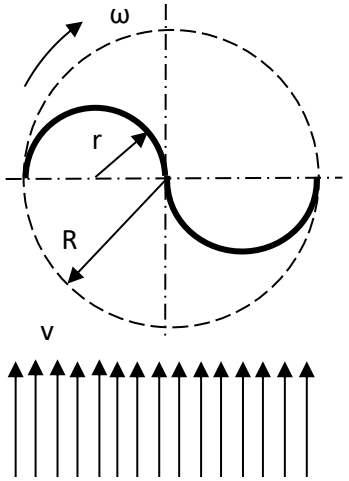

Fig. 2. *Transversal sections through SWT with overlay (o) and gap (g)*

And specific speed (TSR):

$$TSR = \lambda = u/v \quad (7)$$

The extracted power (4) is:

$$P = C_D \frac{1}{2} \rho v^3 (1-\lambda)^2 \lambda A \quad (8)$$

Abbreviations

WT - Wind Tunnel;
EM - Experimental Model;
VAWT - Vertical Axis Wind Turbine;
LED - Light Emitting Diode;
SWT - Savonius Wind Turbine,"S" rotor;
L - Level;
PB - Pair of Blades;
BL - Betz Limit;
TSR - Tip Speed Ratio.

Notations:

v - Speed wind, m/s;
P - Wind power, W;
ρ - Air density, kg/m3;
λ - Specific speed;
r - exterior cup radius, mm;
R - rotation radius, mm;
g - cup thickness, mm;
g - Gap, mm;
o - Overlap, mm;
σ - Solidity;
f - axial turbine frequency, Hz.

2. Experiments

For experimentation in the wind tunnel we used experimental models according to the table (H395 mm, D150 mm).

- savonius model (1L1PB)

- savonius model with a pair of additional semi-cylindrical (Fig. 3) (1L2PB) light pairs, and in which the first PB are placed according to Benesh configuration (g = 15 mm, o = 1/3 of diametral blade projection).

Experiments were performed on a wind tunnel with the characteristics: measure sections 0.5 m x 0.5 m, wind speeds less than 4.5 m/s.

The tests were performed using the free model and the load-coupled model.

Free rotation in the wind was performed using a graphite-bearing device to have minimal mechanical friction.

Experiments on behaviour under mechanical, and electrical load assumed the use of a speed multiplication system (x3.5) and a DC generator (5V).

At the terminals of the generator were connected electric elements and a LED and then electric loads of 1, 1.5 kΩ and 2 kΩ.

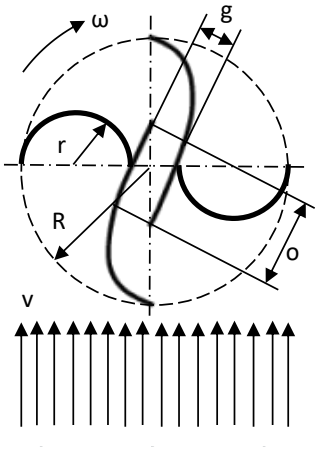

Fig. 3. *Experimental model (transversal section) with a pair of semicilindrical additional blades.*

At the terminals of the generator were connected electric elements and a LED and then electric loads of 1, 1.5 kΩ and 2 kΩ.

For comparison, a SWT model with the same swept area with 1L1PB (one level and one pair of blades) was used.

Experiments are encoded as follows:

- N experimental model without mechanical or electrical loads;

- M-experimental model with mechanical load (speed multiplier and DC generator);

- ML-idem plus LED to indicate working voltage;

- ML1-mechanical load, LED and in parallel a 1kΩ resistor;

- ML1.5-mechanical load, LED and in parallel a 1.5k Ω resistor;

- ML2-mechanical load, LED and in parallel a 2 kΩ resistor.

Obs. For many experiments, the electrical loads on the DC generator of 1.5 kΩ and 2 kΩ were too high and the experimental model did not rotate.

3. Results and discussions

For each model and electrical or mechanical load conditions, measurements were made from the maximum speed to the zero-wind speed and if the pattern did not stop rotating the measurements.

Regarding the movement of the models under the above mentioned conditions, it can be noticed that the models which rotate freely (only mechanical friction in the bearings and the specific friction in the

air) for the same wind speed have x2 to x4 rotation speeds compared to the models with different mechanical loads and / or electric (Fig. 1). The specific speed (λ, TSR) has the same variation: for example, at 4 m/s wind speed, TSR in free models is x4 ... x5 times higher.

The load tests of the experimental models (M, ML, ML1) show the correct behaviour of the models in the sense that as the load increases on the wind turbine experimental model, its speed decreases (Fig. 1) and the TSR (Fig. 2, Fig. 3).

The analysis of the dynamic behaviour was done following the Re number evolution for the experiments performed. (Fig. 7, Fig. 8). It is observed that the higher values Re number to freely rotate experimental models (<85,000) and the values of <30,000 models tested under load.

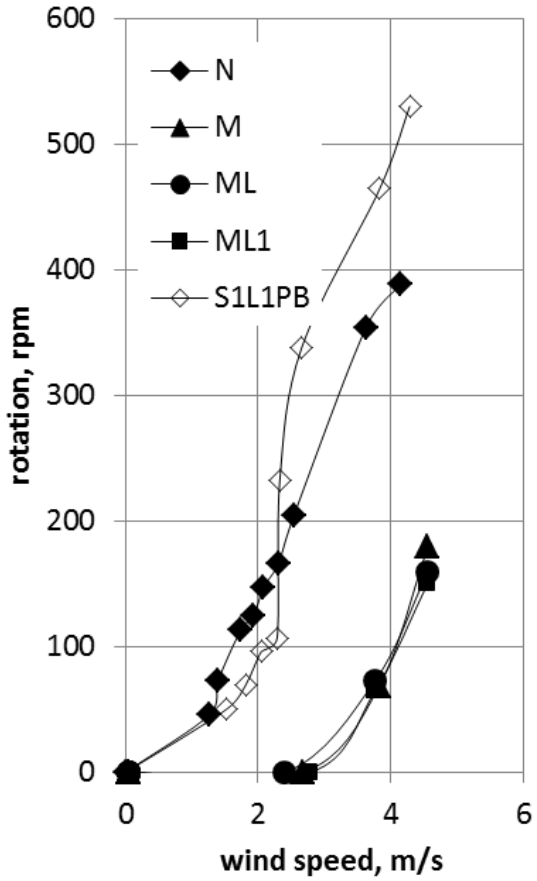

Fig. 4. *Rotations of EM with wind speed*

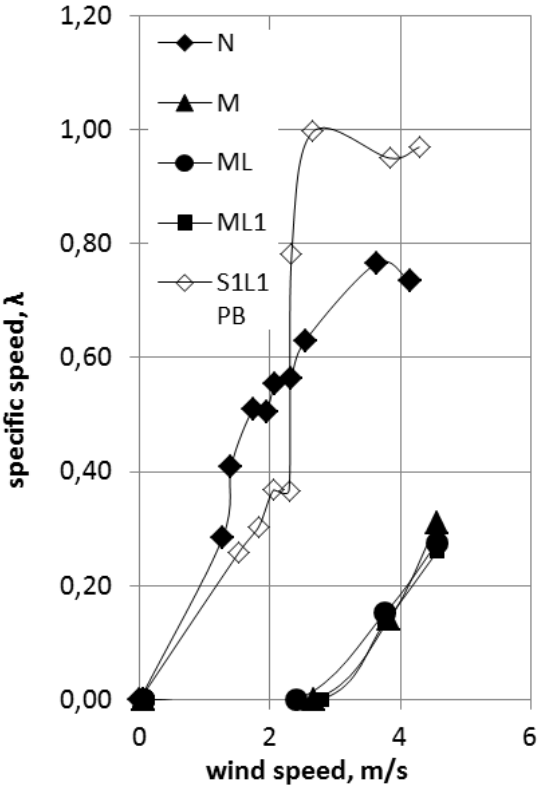

Fig. 5. *Evolution of λ (TSR) with wind speed*

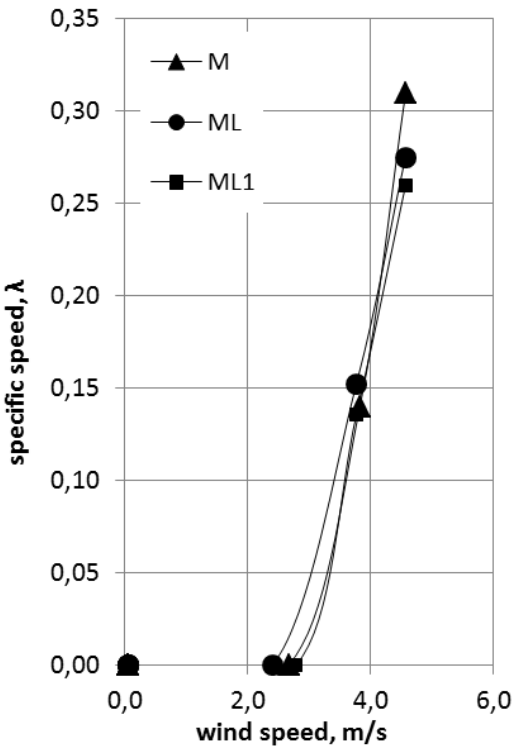

Fig. 6. *TSR (or λ) only for experiments under load*

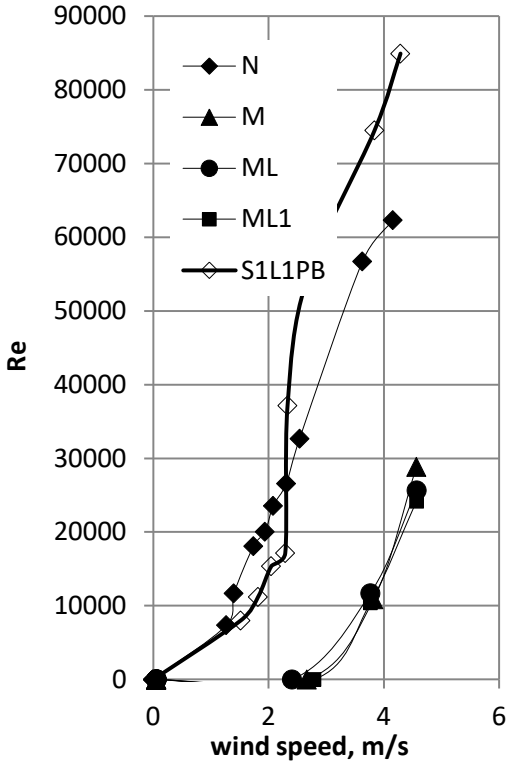

Fig. 7. *Re number with wind speed for all experiments*

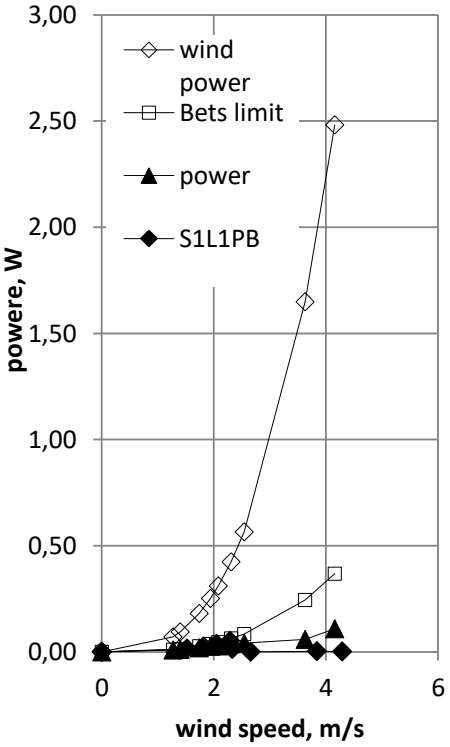

Fig. 9. *Power of models with wind speed versus wind power and Betz limit*

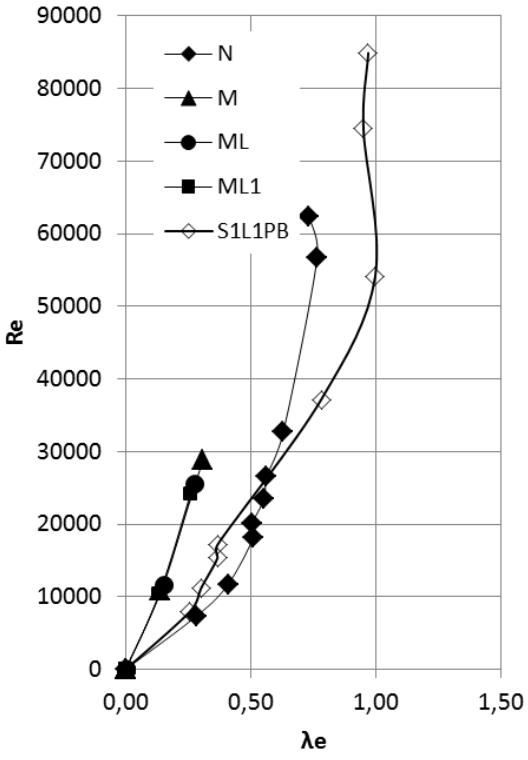

Fig. 8. *Re number variation with TSR of experimental models*

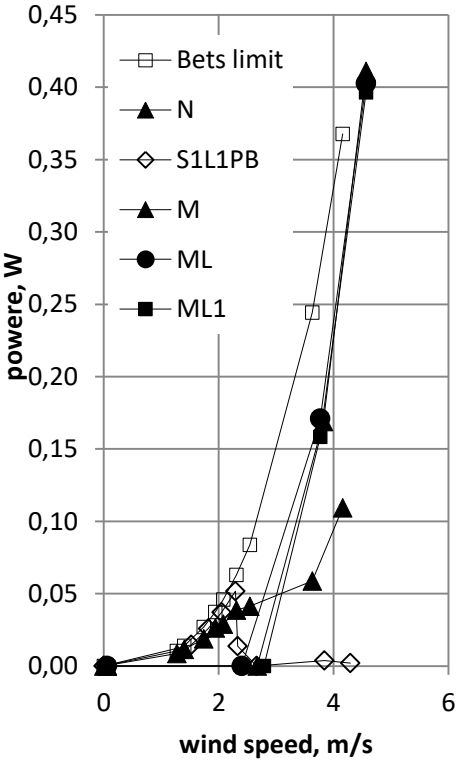

Fig. 10. *Power of experimental models with wind speed under Betz limit*

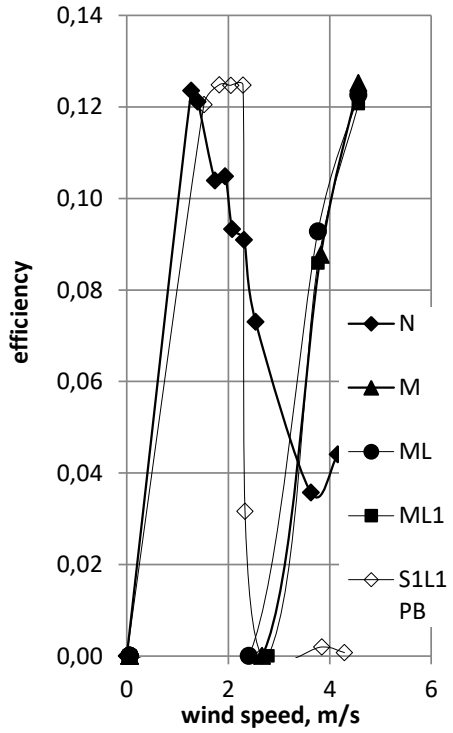

Fig. 11. *Efficiency over experiments with wind speed*

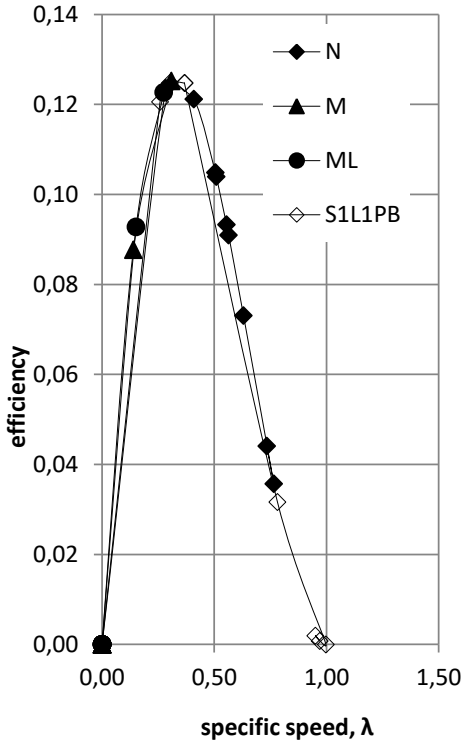

Fig. 12. *Efficiency over experiments with specific speed (TSR, λ)*

Energy efficiency is about 12.5% (Fig. 12). The study of energy efficiency dependency on wind speed (Fig. 11) shows that free models (N, SWT 1L1PB) achieve maximum efficiency at low wind velocities (1.5-2 m/s) and experimental models under load achieve the maximum efficiency at maximum test speeds (4.5-4.6 m/s).

4. Conclusions

Experiments fall within the VAWT theory, i.e.: the extracted power is less than the Betz limit (Fig. 9, Fig. 10) [2, 5].

The increase in load on the experimental wind turbine model with vertical axis (VAWT, Fig. 3) has following effects:

- decreasing TSR (λ) (Fig. 5, Fig. 6);
- Re number down to 30000 at 4.6m / s wind speed (Fig. 7, Fig. 8);
- achieving a maximum efficiency of wind energy conversion at 4.6m / s (Fig. 11);
- maintaining the maximum efficiency of the wind energy conversion to the mechanical and electrical energy at λ = 0.3-0.4 (Fig. 12).

The presence of a pair of additional blades positioned perpendicularly (cross-sectional) on the base pair of blades (Benesh) brings changes to the SWT (1L1PB).

References

[1]. Menet J. L., Bourabaa N., *Increase in a savonius rotor efficiency*.
[2]. Hau Erich, *Wind Turbines, Fundamentals, Technologies, Applications, Economics*, s.l.: Springler, 2006.
[3]. Manwell J. F., McGowan J. G., Rogers A. L., *Wind Energy Explained. Theory, Design And Application*, s.l.: John Wiley & Sons Ltd, p. 590, 2002.
[4]. Smulders P. T., *Rotors for wind power*, Eindhoven: University of Technology, Eindhoven, Faculty of Physics, 1st edition October 1991, (revised edition January 2004).
[5]. Dumitrescu H., Georgescu A., *Calculul elicei, Cap. 4 - Elicea eoliana*, s.l.: Editura Academiei Romane, 1990.
[6]. Manwell J. V., McGowan J. G., Rogers A. L., *Wind Energy Explained. Theory, Design And Application.*
[7]. Benesh A., *Wind turbine system using a vertical axis Savonius-type rotor*, US Patent 4784568, 1988.

MANUSCRISELE, CĂRŢILE ŞI REVISTELE PENTRU SCHIMB, PRECUM ŞI ORICE CORESPONDENŢE SE VOR TRIMITE PE ADRESA:

MANUSCRIPTS, REVIEWS AND BOOKS FOR EXCHANGE COOPERATION, AS WELL AS ANY CORRESPONDANCE WILL BE MAILED TO:

LES MANUSCRIPTS, LES REVUES ET LES LIVRES POUR L'ECHANGE, TOUT AUSSI QUE LA CORRESPONDANCE SERONT ENVOYES A L'ADRESSE:

MANUSCKRIPTEN, ZIETSCHRITFTEN UND BUCHER FUR AUSTAUCH SOWIE DIE KORRESPONDENZ SID AN FOLGENDE ANSCHRIFT ZU SEDEN:

After the latest evaluation of the journals by the National Center for Science Policy and Scientometrics (**CENAPOSS**), in recognition of its quality and impact at national level, the journal will be included in the B^+ category, 215 code (http://cncsis.gov.ro/userfiles/file/CENAPOSS/Bplus_2011.pdf).

The journal is already indexed in:

SCIPIO-RO: http://www.scipio.ro/web/182206

EBSCO: http://www.ebscohost.com/titleLists/a9h-journals.pdf

Google Academic: https://scholar.google.ro

Index Copernicus: https://journals.indexcopernicus.com

The papers published in this journal can be viewed on the website of "Dunarea de Jos" University of Galati, the Faculty of Engineering, pages: http://www.sim.ugal.ro, http://www.imsi.ugal.ro/Annals.html, or at: www.fascicula9.ugal.ro.

Name and Address of Publisher:
Contact person: Elena MEREUȚĂ
Galati University Press - GUP
47 Domneasca St., 800008 - Galati, Romania
Phone: +40 336 130139
Fax: +40 236 461353
Email: gup@ugal.ro

Name and Address of Editor:
Prof. Dr. Eng. Marian BORDEI
"Dunarea de Jos" University of Galati, Faculty of Engineering
111 Domneasca St., 800201 - Galati, Romania
Phone: +40 336 130208
Phone/Fax: +40 336 130283
Email: mbordei@ugal.ro

AFFILIATED WITH:

- THE ROMANIAN SOCIETY FOR METALLURGY
- THE ROMANIAN SOCIETY FOR CHEMISTRY
- THE ROMANIAN SOCIETY FOR BIOMATERIALS
- THE ROMANIAN TECHNICAL FOUNDRY SOCIETY
- THE MATERIALS INFORMATION SOCIETY (ASM INTERNATIONAL)

Edited under the care of the FACULTY OF ENGINEERING

Annual subscription (4 issues per year)

Editing date: 15.06.2018
Number of issues: 200
Printed by Galati University Press (accredited by CNCSIS)
47 Domneasca Street, 800008, Galati, Romania